A NEW MINERALOGICAL APPROACH TO PREDICT THE

COEFFICIENT OF THERMAL EXPANSION

OF AGGREGATE AND CONCRETE

A Thesis

by

SIDDHARTH NEEKHRA

Submitted to the Office of Graduate Studies of
Texas A&M University
in partial fulfillment of the requirements for the degree of

MASTER OF SCIENCE

December 2004

Major Subject: Civil Engineering

A NEW MINERALOGICAL APPROACH TO PREDICT THE

COEFFICIENT OF THERMAL EXPANSION

OF AGGREGATE AND CONCRETE

A Thesis

by

SIDDHARTH NEEKHRA

Submitted to the Texas A&M University
in partial fulfillment of the requirements
for the degree of

MASTER OF SCIENCE

Approved as to style and content by:

Dan G. Zollinger (Chair of Committee)	Robert L. Lytton (Member)
Charles W. Graham (Member)	David V. Rosowsky (Head of Department)

December 2004

Major Subject: Civil Engineering

ABSTRACT

A New Mineralogical Approach to Predict the Coefficient of Thermal Expansion of

Aggregate and Concrete. (December 2004)

Siddharth Neekhra, B.E., Government Engineering College Raipur

Chair of Advisory Committee: Dr. Dan G. Zollinger

A new mineralogical approach is introduced to predict aggregate and concrete coefficient

of thermal expansion (CoTE). Basically, a modeling approach is suggested based on the

assumption that the CoTE of aggregate and concrete can be predicted from the CoTE of

their constituent components. Volume percentage, CoTE and elastic modulus of each

constituent mineral phase are considered as input for the aggregate CoTE model, whereas

the same properties for coarse aggregate and mortar are considered for the concrete CoTE

model. Methods have been formulated to calculate the mineral volume percentage from

bulk chemical analysis for different type of rocks commonly used as aggregates in Texas.

The dilatometer testing method has been established to measure the CoTE of aggregate,

pure minerals, and concrete. Calculated aggregate CoTE, based on the determined CoTE

of pure minerals and their respective calculated volume percentages, shows a good

resemblance with the measured aggregate CoTE by dilatometer. Similarly, predicted

concrete CoTE, based on the calculated CoTE of aggregate and mortar and their

respective volume percentages compares well with the measured concrete CoTE by

dilatometer. Such a favorable comparison between predicted and measured CoTE

provided a basis to establish the composite model to predict aggregate and concrete

CoTE. Composite modeling will be useful to serve as a check of aggregate source

variability in terms of quality control measures and improved design and quality control measures of concrete.

DEDICATION

This thesis is dedicated to my parents for their constant support, love and sacrifice.

ACKNOWLEDGEMENTS

First, I would like to thank Dr. Dan G. Zollinger, without whose support and trust I wouldn't have been able to finish this work. I will never forget the good time I had working with him. I can not find enough words to convey my gratitude towards him. I would also like to thank Dr. Robert L. Lytton and Dr. Charles W. Graham for their time and support as committee members.

I would like to thank Dr. Anal Mukhopadhyay for his valuable advice and guidance during my research.

This research was sponsored by the Texas Department of Transportation. I would like to gratefully acknowledge the financial support of TxDOT.

I would like to acknowledge the help of the Texas Transportation Institute (Texas A&M University) lab staff especially Gerry Harrison for his help during the research.

Along with these people there were several others who were always with me just in case I needed some help of any kind. This includes my friends at Texas A&M University and back in India.

Finally, I would like to thank my family back at home. Their constant encouragement, love and support kept me focused toward successful completion of this thesis.

TABLE OF CONTENTS

LIST OF FIGURES

LIST OF TABLES

1. INTRODUCTION

OBJECTIVE

Aggregate properties play a very important role in the performance of continuously reinforced concrete pavement (CRCP) pavements. In a continuously reinforced concrete pavement, the key element to developing a uniform crack pattern is maintaining a balance between the following aggregate factors that affect pavement performance:

- concrete, aggregate/paste early-age bond strength
- concrete drying shrinkage and creep
- aggregate coefficient of thermal expansion (CoTE)
- concrete strength
- modulus of elasticity, and
- aggregate type, gradation, and blend effects.

The present study focused on the role of aggregate CoTE. The coefficient of thermal expansion is a length change in a unit length per degree (Celsius/Fahrenheit) temperature change.

Most paving materials experience a change in volume due to a change in temperature, and this dependency is described in terms of CoTE. Concrete is not an exception to this and its CoTE depends on the thermal behavior of the individual components (i.e., coarse aggregate, fine aggregate and cement paste). The type of coarse and fine aggregate and the mixture proportion play an important role in the final CoTE of the concrete (*1*).

This thesis follows the style of *Transportation Research Board.*

During the past decades several researchers have shown that the thermal properties of cement, mortar, and aggregates can affect the thermal behavior of concrete (*2*). The CoTE of the aggregate determines the thermal expansion of concrete to a considerable extent because the aggregate composes of about 70-75 percent of the total solid volume of the mixture. The aggregate also governs the degree of physical compatibility of the components as the temperature changes (*3*).

Pavement distresses such as punchouts, faulting, corner breaks, and possibly spalling are related to the thermal expansion properties of concrete (*4*). It has been suggested that if the CoTE of the coarse aggregate and of the hydrated cement paste are very different, a large change in temperature may introduce differential movement and thus causing debonding (*5*). Therefore, characterization of key aggregate properties will enable the projection of behavior of concrete with reasonable accuracy, which in turn may result in improved understanding of pavement behavior and the effect of the material, thermal spacing on performance.

Role of Aggregate Coefficient of Thermal Expansion on CRC Pavement Performance

The coefficient of thermal expansion of concrete is related to the volumetric change hardened concrete undergoes as a result of temperature change. It certainly plays a role in the thermal induced opening and closing of transverse cracks. The two main constituents of concrete, cement paste and coarse aggregate (which have dissimilar thermal coefficients), combine to form a composite coefficient of thermal expansion of concrete. Since more than half of the concrete volume is coarse aggregate, the major factor influencing the coefficient of thermal expansion of concrete appears to be the type of coarse aggregate. Studies conducted by Brown (*6*) and later by Won et al. (*7*) showed that the effect of silica content

in the aggregate on the CoTE of the concrete is significant. This study indicated that the higher the silica content, the higher the CoTE. Thermal effects are manifested in the daily variation in the opening and closing of transverse cracks. This opening and closing contributes to the stress in the reinforcing steel, but only to the extent that the CoTE of the steel reinforcement is greater than the CoTE of the concrete. Consequently, the effect due to the reinforcing steel stress is often much lower than the effect due to drying shrinkage. However, the opening and closing of cracks is a factor in performance, since the degree of load transfer is directly related to the width of the cracks. Therefore, crack widths should be restricted within certain limits.

Several researchers have determined the coefficient of thermal expansion of various aggregates and their results indicate that the coefficient of thermal expansion varies widely among different aggregates, both with mineralogical content and with geographic location. Some siliceous aggregates exhibit higher thermal expansion properties and have CoTE values as high as $13 \times 10^{-6}/^{\circ}C$, whereas some limestone aggregates exhibit expansion values lower than $6 \times 10^{-6}/^{\circ}C$ (*3, 5, 8, 9*). Siliceous aggregates such as chert, quartzite, and sandstone have CoTE that range between $10 \times 10^{-6}/^{\circ}C$ to $12 \times 10^{-6}/^{\circ}C$, while basalt, granite, and gneiss CoTE may vary between $6 \times 10^{-6}/^{\circ}C$ to $9 \times 10^{-6}/^{\circ}C$. CoTE values for limestone aggregates are typically less than granite or basalt. Measured CoTE values of granite range between $8 \times 10^{-6}/^{\circ}C$ to $9 \times 10^{-6}/^{\circ}C$, while the CoTE for basalt is typically slightly higher than that of granite. The data have also demonstrated that aggregates of the same type and from the same source may vary significantly in CoTE values.

CoTE characterization of an assorted mixture of aggregates will need improvement in order to better understand the behavior patterns of concrete structures and concrete

pavements made with these different types of aggregates. It is anticipated that an estimated value of the CoTE for concrete may be calculated from the weighted averages of the coefficients of the aggregates and the hardened cement paste. Furthermore, the coarse aggregate is expected to have the dominant effect upon the thermal expansion behavior of concrete, as previously discussed. It has also been noted that concrete containing well-graded aggregates has higher coefficient of thermal expansion values than concrete containing gap-graded aggregates. The thermal behavior of the coarse aggregate may play a greater role in the opening and closing of cracks after creep effects of concrete are diminished due to aging and maturing of the concrete.

METHOD OF APPROACH

The available test data (*5, 9*) indicates that CoTE varies widely among different aggregates with differing mineralogical content and geographical location. Since aggregates are composite materials consisting of different minerals in different proportions, it is assumed that their properties can be determined from the properties of their component minerals (*10*). In this context, a new mineralogical approach to model aggregate CoTE, a composite model to predict aggregate CoTE from the CoTE of constituent minerals and their respective volume percentages is introduced. Similarly, concrete CoTE can be modeled using the CoTE of constituent coarse aggregate and mortar. Validation of this composite model can be established by drawing favorable comparisons between calculated and measured CoTE. We use the volumetric dilatometer (*11*) to measure the CoTE of minerals, aggregates and concrete in this context. The Volumetric dilatometer (Figure 1) is an apparatus used to determine the bulk coefficient of thermal expansion of coarse aggregate, fine aggregate and concrete.
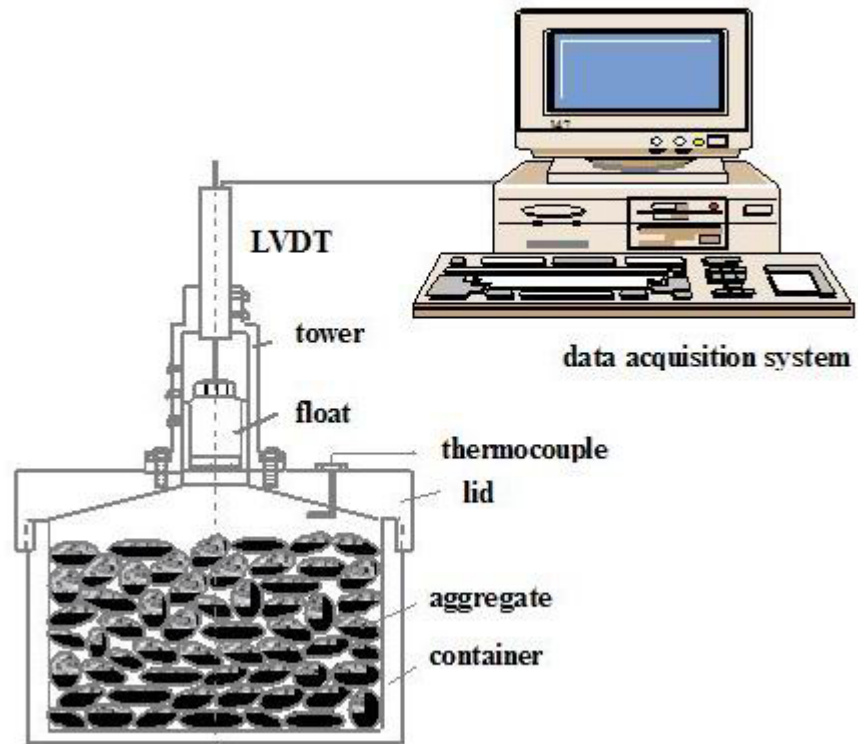
Figure 1 Dilatometer Device.

2. LITERATURE REVIEW OF AGGREGATE AND CONCRETE CoTE

The role of physical, mechanical, and chemical properties of coarse aggregates on the behavior and performance of paving concrete are often described in terms of their effects on concrete strength, shrinkage, creep, and bond strength. Specific aggregate properties are listed in Table 1 relative to their physical attributes. These physical attributes can be related to concrete mixing, placing, finishing, hardening, and other construction and pavement related characteristics. The mechanical properties of an aggregate predict its ability to resist loads and stresses. The chemical properties of an aggregate are a result of its chemical composition. Aggregate's chemical interaction with concrete pore solution and water depends on its chemical properties. CoTE is classified as mechanical property of aggregate.

Table 1 Aggregate Properties.

Physical	Mechanical	Chemical
Particle shape	Strength	Solubility
Maximum particle size	Elastic modulus	Base exchange
Surface texture	Coefficient of thermal expansion	Surface charge
Percent voids	Resilient modulus	Chloride content
Thermal conductivity	Resistance to loads	Reactivity
Permeability	Resistance to degradation	Slaking
Specific gravity		Coatings
Porosity		Oxidation potential
Gradation		Resistivity

AGGREGATE COEFFICIENT OF THERMAL EXPANSION

As already mentioned earlier, aggregate CoTE is one of the most important behavioral characteristics of an aggregate material, which is found to influence the performance of concrete pavement primarily due to its effect on dimensional change under a change in temperature. The CoTE of an aggregate has a marked effect on the CoTE of concrete containing the given aggregate. Some of the pavement distresses are related to the thermal expansion properties of jointed concrete (*4*), but the more pronounced effect is on the development of the crack pattern and the daily and seasonal temperature changes on the width of transverse cracks in CRC pavements, as it would affect their load transfer efficiency.

Pavements are susceptible to bending and curling caused by temperature gradients that develop when concrete is cool on one side and warm on the other (4). Moisture and temperature variations cause volumetric changes that can lead to cracking and premature failure in Portland cement Concrete (PCC) pavements. In jointed pavements, the volumetric changes caused by friction between the concrete and the base can lead to transverse cracks that can adversely affect load transfer and carrying capacity. Knowledge of this property during the design stage of pavement before the construction allows for accurate prediction of the potential thermal change on crack development and crack width and enhances the overall design process. Siliceous gravel use results in larger crack width than does the limestone and at low temperature of pavement this difference is higher (1) as shown in Figure 2. These results provide an idea of how to classify aggregate based on their CoTE values. Aggregate CoTE is divided into three categories (Table 2) based on their effects on concrete performance**.**
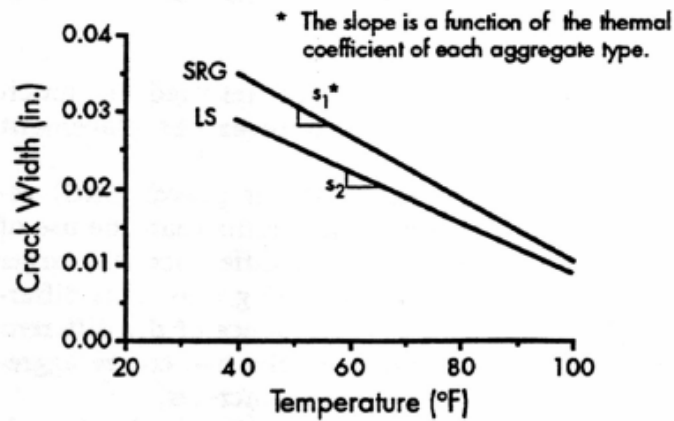
Figure 2 Effect of CoTE of Slab Temperature on Crack Width (*1*).

Table 2 Aggregate CoTE Classification.

Category	CoTE (10^{-6}/°C)
Low	<6
Medium	6-9
High	>9

As previously discussed, the aggregate coefficient of thermal expansion is a function of its mineralogical composition. This aspect is described below in detail.

Chemical and Mineralogical Aspects of Aggregate CoTE

Hardened concrete has a coefficient of thermal expansion greater than that of aggregate, but the expansion of concrete is proportional to that of the aggregate, as aggregates form a major part of the concrete (*5*). Aggregates commonly used in concrete are classified into three major categories: igneous, sedimentary, and metamorphic rocks. These groups can be further divided into subgroups depending on their chemical and mineral composition and their textural and internal structure. Research suggests that a definable relationship exists between the chemical and mineral composition of the aggregate and its measured CoTE. In

order to develop this relationship to modeling stage a better understanding of the mineralogical composition in relation to the chemical oxide composition of aggregate is warranted. Accurate knowledge of an aggregate's mineral composition is the key to the prediction of thermal change resulting from a change in temperature.

Igneous rocks are the result of solidification of molten material that originated in the earth's interior. Magma that flows out onto the earth's surface and cools rapidly forms volcanic rocks such as basalt, rhyolite, andesite, etc. Those that do not reach the surface and solidify slowly in the subsurface from plutonic rocks, e.g. granite, diorite, gabbro, ultrabasic rocks etc. Igneous rocks can be subdivided into three groups based on chemical composition: acidic, intermediate, and basic. Rocks rich in SiO_2 are termed acidic and those less rich in SiO_2 are termed basic. Acidic rocks contain sufficient silica for the mineral quartz to be present. Basic rocks, on the other hand, do not have sufficient silica to contain quartz. Less silica is found in feldspars, which contain other cations: Al, Na, K, and Ca. Other elements, Mg and Fe in particular, are components of olivines, pyroxenes, and amphiboles. Certain minerals are frequently found together: for example, olivine, pyroxene, and calcium plagioclase (anorthite). Others such as quartz and olivines never appear together. There exists an approximate inverse correlation between the temperatures at which a mineral crystallizes from magma and its relative resistance to alteration processes that affect all igneous rocks. Olivine and pyroxenes, for example, are minerals formed at high temperatures and are easily altered. At the other extreme, quartz resists most alteration processes.

Most common sedimentary rocks are formed by weathering of pre-existing rocks (sedimentary, igneous, and metamorphic), transport of weathered products by such means

as wind and moving water, deposition of suspended materials from air or water, compaction, and digenesis. Sedimentary rocks are also formed through chemical process such as dissolution and precipitation of minerals in water and secretion of dissolved minerals through organic agents.

Metamorphic rocks are formed by a process called metamorphism (i.e., during burial or heating, where rocks experience recrystallization and mutual reaction of constituent minerals as their stability fields are exceeded). Because these reactions take place without ever reaching the silica melt phase, they are called metamorphic. After formation, most rocks are exposed to a series of processes and cannot be classified by a single process.

The variation of the CoTEs of the different types of aggregates can be explained by the presence and proportions of different types of minerals they contain. It is true that different rock types commonly used as aggregates have their characteristic chemical compositions. Therefore, differences in chemical composition should ultimately reflect in different mineralogy. The chemical composition will change if the rock types change. Aggregate from the same source could have slightly different coefficients of thermal expansion because of slight variations in mineralogy or textural features like recrystallization, crystallinity, etc.

PREVIOUS METHODS OF TESTING FOR AGGREGATE AND CONCRETE CoTE

Many attempts have been made to measure the coefficient of thermal expansion of aggregates and concrete. Researchers have tried a number of different approaches, ranging from using strain gages (to measure length change) to measurement of the volume change

of a collective sample. The majority of these test methods are based on the measurement of linear expansion over a temperature range. However, determining the linear expansion of fine aggregate is not possible because of the smaller size of particles. The method explained by Willis and DeReus (*12*) allows measurements to be made over a considerable particle size range using an optical lever. The specimens used by Willis and DeReus were 25.4 mm diameter cores, 50 mm long, drilled from the aggregate specimen to be tested and placed in a controlled-temperature oil bath with a range of $2.78 \pm 1.7^{\circ}C$ to $60 \pm 2.8^{\circ}C$. When the temperature is varied the vertical movement of the specimen was measured by observing through a precise level the image, reflected by mirror of optical lever, having 25.4 mm lever arm, on a vertical scale placed 6.1 m from the mirror. The calculated coefficients of thermal expansion are probably accurate to $\pm 3.6 \times 10^{-6}/^{\circ}C$ by using the method.

In the strain gage test method, developed by the U.S. Army Corps of Engineers (*13*), electrical resistance wire strain gages measure the coefficient of thermal expansion of coarse aggregate. The apparatus consists of

- a controlled-temperature cabinet,
- a SR-4 strain indicator,
- resistance electrical strain gages,
- suitable cement for attaching the gages to the specimens,
- a multipoint recording potentiometer,
- a standard specimen of known coefficient of thermal expansion,
- a switchboard with silver-contact switches in circuit with the SR-4 indicator,
- individual lead wires to the panel board,

- a panel board built for mounting specimens with gages attached through binding posts to the lead wires,

- thermocouples for temperature measurements within a cabinet at various points, and

- a diamond cutoff wheel for sawing specimens.

The strain is measured in three mutually perpendicular directions in the specimen. Specimens of coarse aggregate are selected in a size that permits preparation of surfaces SR-4 strain gages mounting. The SR-4 strain gages are attached using only enough cement to completely coat the gage and specimen surfaces to be joined. After a curing period, the specimens are mounted on the panel board along with the standard sample. The temperature is set to 135°F and is maintained until equilibrium is reached. After equilibrium, each gage, including the standard gage, is read. The temperature setting is then changed to 35°F and as soon as possible after the equilibrium is attained, readings are taken again. This procedure is repeated for at least 10 cycles. The reading from the first cycle is discarded. The calculation is made as follows:

$$C = 4.3\ \Delta t - (\Delta y + \Delta x) / \Delta t \qquad\qquad (1)$$

where, C = linear coefficient of thermal expansion,
  4.3 = linear coefficient of thermal expansion of quartz $(10^{-6}/^{\circ}\text{F})$,
  Δt = temperature difference between successive readings$(^{\circ}\text{F})$,
  Δy = difference between successive readings of standard gage $(10^{-6}\ \text{inch/inch})$, and
  Δx = difference between successive readings of test gage $(10^{-6}\ \text{inch/inch})$.

Venecanin (*14*) reported a similar but more elaborate setup, where strain gages were mounted to obtain measurements parallel to the edges and in both diagonal directions on each of six faces of a cube of rock.

The main drawback of using strain gages is that they cannot be used on material with different sizes and shapes. Creep of gages cemented to the surfaces can occur during the test and cause errors in gage readings. Because of the size and usually heterogeneous nature of fine aggregate, none of the preceding methods are readily adaptable to the determination of the CoTE of this type of material. The usual approach has been to determine the linear expansion of mortar bars containing the fine aggregate. However, the results obtained include the effects of the length change contributed by the cement.

Mitchell (*15*) described a method in which specimens of 25.4 to 76.2 mm in size were coated with wax and held in fulcrum-type extensometer frames. The specimens were immersed in a circulating ethylene glycol solution held at a desired temperature, and electromagnetic strain gages with electronic indicators were used for measurement.

The dilatometer method was devised in 1951 by Verbeck and Haas to measure the coefficient of volumetric thermal expansion of aggregate (*16*). Their apparatus consisted of a 1 Liter dilatometer flask to which was attached a laboratory-constructed capillary bulb arrangement containing electrical contacts (Figure 3). In operation, the flask was filled with aggregate and water then the apparatus was allowed to equilibrate at one of the controlling electric contacts. The equilibrium temperature was measured with a Beckman thermometer. Verbeck and Haas calculated the coefficient of thermal expansion on the basis of the temperature required to produce an expansion equivalent to the volume between the equilibrating electrical contacts. The apparatus needed to be calibrated to determine the coefficient of volumetric thermal expansion of the flask. The aggregate sample was immersed in water for a few days in order to remove any air present. The temperature increment was approximately 4°C; however, this varied depending on the temperature at

which the flask was operated, the ratio of the volume increment between the contacts to the flask volume, the amount of aggregate in the flask, and the thermal characteristics of the aggregate. For measurements made below the freezing point of water, a non-reactive liquid, such as toluene, which does not freeze at the desired temperature, could be substituted. It was fairly easy to prepare the sample for the experiment. In comparison to other methods, such as a mounted strain gage on a specific rock sample, this method has the advantage of testing aggregates of different sizes.

A test method was recently developed by the American Association of State Highway and Transportation Officials (AASHTO) as test number TP60-00, "Standard Test Method for the Coefficient of Thermal Expansion of Hydraulic Cement Concrete"(*17*). The procedure requires a 4 inch diameter core, cut to a length of 7 inches (Figure 4). The sample is saturated for more than 48 hours and then subjected to a temperature change of 40°C in a water bath. The length change of the specimen is measured and, with the known length change of the measuring apparatus under the same temperature change, the CoTE of the concrete specimen can be determined.
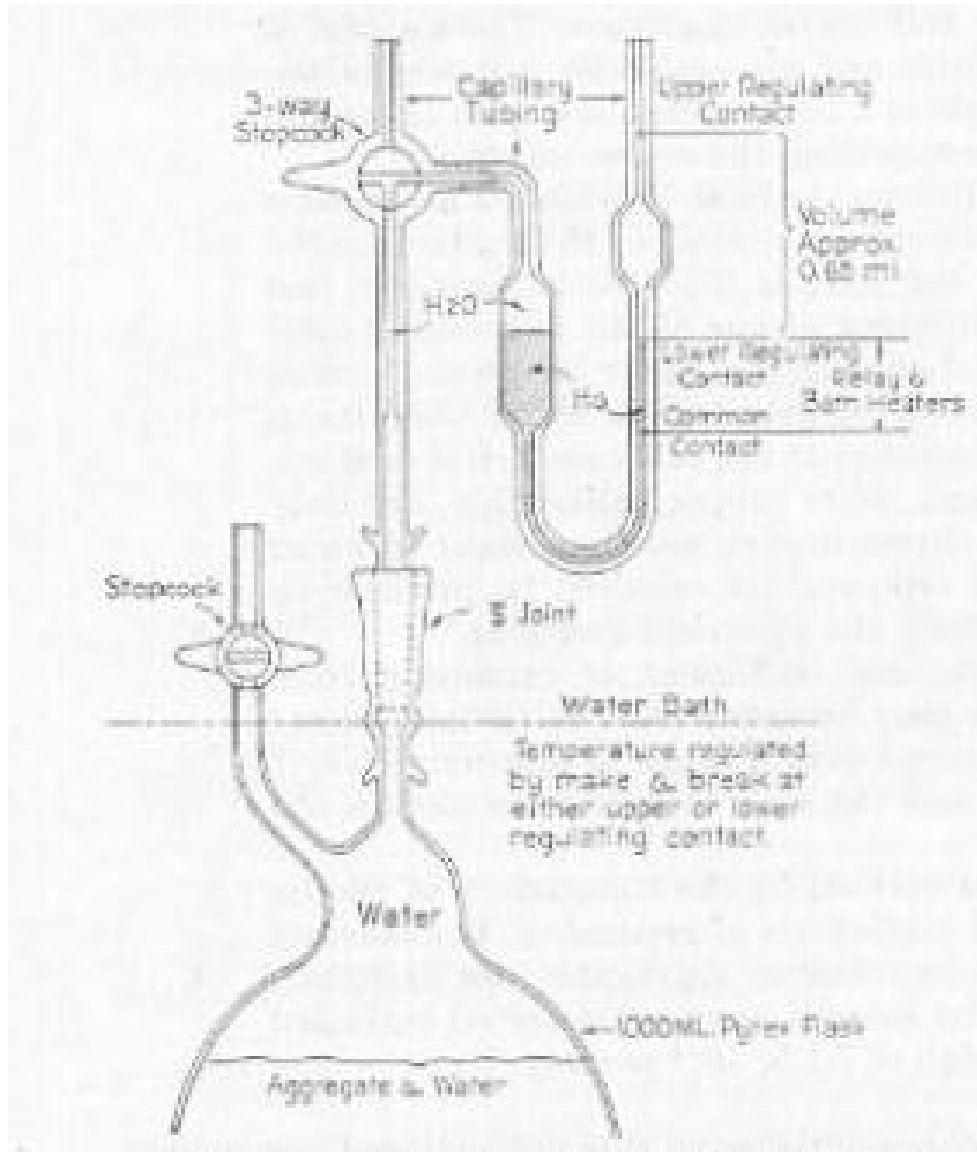
Figure 3 Dilatometer Developed by Verbeck and Haas (*16*)
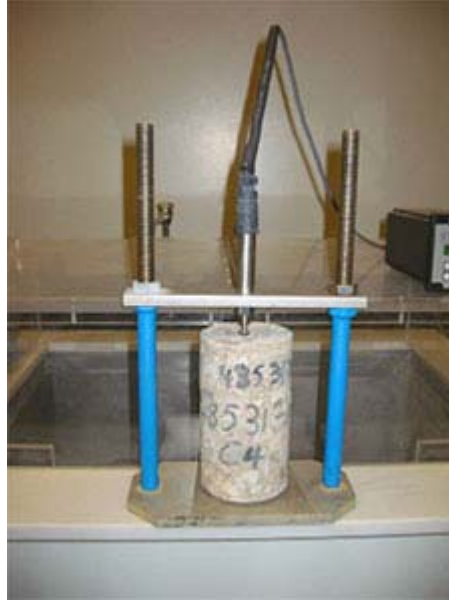
Figure 4 Concrete Specimen for Standard Test Method for the Coefficient of Thermal Expansion of Hydraulic Cement Concrete (*17*).

A computer program, CHEM2 (*18*), was developed by the Center for Transportation Research, The University of Texas at Austin, Texas, which allows the researcher to estimate the properties of concrete compressive strength, coefficient of thermal expansion, splitting tensile strength, elastic modulus, and drying shrinkage for curing times ranging from 1 to 28 days using input of aggregate bulk chemical analysis results. The methodology of the CHEM2 program is such that it first identifies the type of aggregate and then predicts the performance using a model prepared for that type of aggregate. The program either identifies the aggregate from either the user input or the bulk chemical analysis results.

CHEM2 is based on regression analysis of the oxide weight percentage of the aggregate to predict concrete properties independent of concrete mixture proportions. This program predicts mineral weight percent of all types of aggregates based on a common set of chemical formulae.

GNOMIX PVT HIGH PRESSURE DILATOMETER (*19*)

Dilatometry measures the change in volume of a specimen subjected to different temperatures and pressures. The Gnomix PVT Apparatus (Figure 5) generates pressure-specific volume-temperature measurements using high-pressure dilatometry.

Approximately 1 gram of dry sample is loaded into a sample cell, and placed in the PVT apparatus. The machine is brought to just below the melting point temperature, Isothermal data acquisition begins as soon as the machine is brought at this temperature. Volume readings are taken by an LVDT for the specified temperature at pressures ranging from 10-200 MPa. The procedure is repeated for decreasing temperatures, down to ambient temperature. Data may also be gathered while heating the specimen. From the gathered data, the volumetric expansion coefficient in the solid state is extracted.

Figure 5 Gnomix pvT High Pressure Dilatometer (19).

3. CoTE LABORATORY TESTING AND MODEL DEVELOPMENT

VOLUMETRIC DILATOMETER METHOD

During the present study Volumetric Dilatometer (*11*) method was used to measure the

CoTE of both coarse and fine aggregate as well as pure minerals, metals, and glass.

Substantial modification in the design of the dilatometer was made in comparison with the

earlier version that Verbeck and Haas used, though the basic working principle remains the

same. The present data acquisition system is also entirely different than with Verbeck and

Hass's model.

TESTING APPARATUS AND CALIBRATION

During this study a test apparatus referred to as a volumetric dilatometer for determining

the bulk coefficient of thermal expansion of both fine and coarse aggregates is used for

verification of model for aggregate and concrete coefficient of thermal expansion. The

method is particularly adaptable to the study of field-saturated coarse aggregates, sand and

concrete cores and provides a means of testing a representative sample of a heterogeneous

coarse aggregate.

Testing Apparatus

The dilatometer test device (Figure 6) consists of a stainless steel container, a brass lid with

hollow tower, a glass float (to which a linear variable differential transducer [LVDT] is

attached), a thermocouple, and a data acquisition system. The inner surface of the lid is

configured at a certain angle so that entrapped air bubbles can easily move along the

surface. A transparent window with graduations at different heights is placed along the side

of the tower to set the water level.
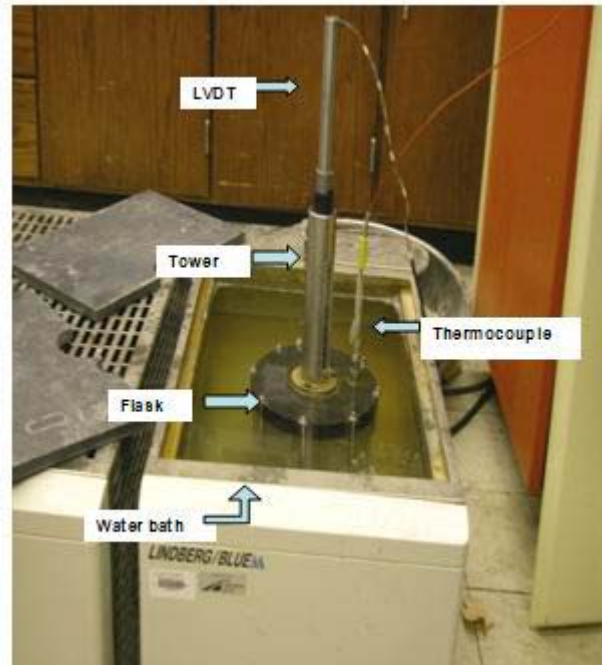
Figure 6 The Dilatometer Test Device.

The dilatometer container is filled with aggregate sample and water. The water surface is filled to a certain fixed graduation mark in the tower. The dilatometer with sample and water inside is placed in a water bath and allowed to experience temperature change through controlling the temperature of water bath. Displacement of water due to thermal expansion of both tested material and water is recorded by the LVDT through the movement of the float, which is placed on the water surface in the tower. Electrical signals are generated by the LVDT as the core moves. The signals are acquired and amplified by a signal conditioner and then recorded by a computer data acquisition system. The LVDT used is a UCAS/sCHAEVITZ model MHR .050, which emits 10.00 V for a displacement of 1.27 mm (0.050 inch) which provides sufficient accuracy in the measurement of volume changes in the small area of the water surface in the tower. A thermocouple is immersed in the water to monitor the temperature inside the container. The temperature and LVDT signals are continuously recorded by the same computer data acquisition system.

Dilatometer CoTE measurement is basically an estimation of the CoTE of the tested material based on the volumetric relationships between water, tested material, and container under a given temperature change. Research has shown that the linear CoTE of an isotopic material is one-third the volumetric CoTE, (Appendix A) and for simplicity, the same is assumed for all tested materials.

Figure 7 represents the initial and final states of a dilatometer test. The container is filled with water and test sample so that the total initial and final volumes, V_1 and V_2, consist of the volume of water, V_w, and volume of aggregate sample, V_a, at each state. The instrument test system measures the displacement of water level, Δh, in the container tower with the change of temperature. These measurements produce an estimation of the coefficient of thermal expansion of aggregate sample based on the volumetric relationships between water, aggregate, and container at a given temperature change.
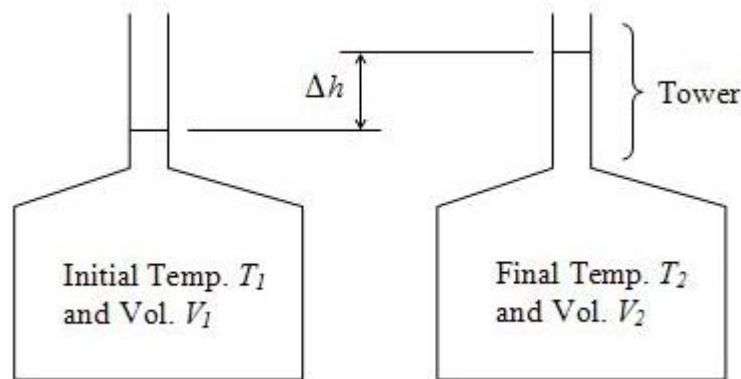
Figure 7 Initial and Final Stages of Dilatometer Testing.

In operation, the container is placed in the water bath and heated by the water surrounding it. When the temperature is raised from T_1 to T_2, the aggregate, the water, and

the container all expand. Therefore, the apparent volume change that the LVDT detects consists of three parts:

$$\Delta V_1 = A \, \Delta h = \Delta V_a + \Delta V_w - \Delta V_f \qquad (2)$$

where　　　　ΔV_1 =　observed total volumetric increase due to temperature change ΔT,

　　　　　　A = inner sectional area of tower,

　　　　　　Δh = rise of the water surface inside the tower,

　　　　　　ΔV_w = volumetric increase of water due to temperature ΔT,

　　　　　　ΔV_f = volumetric increase of inside volume of the dilatometer due to ΔT,

　　　　　　ΔV_a = volumetric increase of aggregate V_a due to ΔT, and

　　　　　　ΔT = temperature increase from T_1 to T_2.

Since　　　　　　　　　　$$V_f = V_a + V_w = V \qquad (3)$$

$$\Delta V_a = V_a \, \gamma_a \, \Delta T$$

$$\Delta V_f = V \, \gamma_f \, \Delta T$$

$$\Delta V_w = V_w \, \gamma_w \, \Delta T = (V - V_a) \, \gamma_w \, \Delta T$$

where　　　　V　=　total inner volume of the flask,

　　　　　　V_w　=　volume of water in the flask,

　　　　　　V_f　=　volume of the flask,

　　　　　　V_a　=　volume of aggregate in the flask,

　　　　　　γ_a　=　coefficient of volumetric thermal expansion of aggregate,

　　　　　　γ_w　=　coefficient of volumetric thermal expansion of water, and

$$\gamma_f \quad = \quad \text{coefficient of volumetric thermal expansion of flask,}$$

We have

$$\gamma_a = \frac{1}{V_a}\left(\frac{A \cdot \Delta h}{\Delta T} - V_a \cdot \gamma_w - (\gamma_w - \gamma_f)(V_w + V_a)\right) \tag{4}$$

The coefficient of thermal expansion of aggregate sample is calculated by equation (4). Among the parameters on the right-hand side of the equation, the cross-sectional area of the tower, A, is fixed known value for a dilatometer. The thermal coefficient of container, γ_f, is also regarded as a fixed value. Other parameters, Δh, ΔT, V_w, V_a, and γ_w, are variable and they are measured in the test or determined by applied test conditions. Close review of the determination of the above input values will help clarify the validity of equation (4).

Initial Total Volume

The initial total volume, V, consists of the volume of water and the volume of the aggregate. This initial total volume is equivalent to the initial volume of the dilatometer, V_f. The initial total volume, V or V_f, is determined by measuring the weight of the dilatometer filled with water at a fixed level. The initial total volume is now determined by multiplying the weight of water and the specific volume of water at the initial temperature (T_1). The weight of water is independent of temperature. Estimation of the specific volume of water at different temperatures is described later in the section in the discussion of the coefficient of thermal expansion of water.

CALIBRATION OF APPARATUS

The dilatometer is calibrated to separate the volumetric expansion of the water and the container from the volumetric expansion of tested material.

The Coefficient of Thermal Expansion of the Dilatometer

The purpose of calibration of the dilatometer is to determine the apparent coefficient of volumetric thermal expansion of the flask and to ensure that the variability from test to test is within acceptable limits. The calibration procedure is described in Appendix B in the form of a calibration protocol. The dilatometer is filled with distilled water and tested over a temperature range from 10^0C to 50^0C in order to estimate the CoTE of the dilatometer container. In this case, the volumetric relation shown in equation (4) becomes

$$\gamma_f = \gamma_w - \frac{A \cdot \Delta h}{V} \cdot \frac{1}{\Delta T} \qquad (5)$$

where $\quad V = V_f = V_w$ and
$\quad\quad\quad V_a = 0$.

This calibration gives an apparent coefficient of thermal expansion of the dilatometer of 5.3×10^{-5} $^\circ$C ± 0.04101 over the temperature range used for the calibration, the volumetric expansion of the dilatometer showed linear behavior; therefore, this value is regarded as a constant.

The Coefficient of Thermal Expansion of Water

The volume change of water is known to be non linear with respect to temperature changes. Therefore, the thermal coefficient of water, γ_w, is variable with respect to the selected temperature for a test. This variable parameter γ_w can be determined from the density of water at different temperatures (*20*) and is presented in Table 3.

Table 3 Densities of Water at Different Temperatures (*20*).

Temperature (°C)	Density (g/cm³)	Temperature (°C)	Density (g/cm³)
0	0.99984	60	0.98320
10	0.99970	70	0.97778
20	0.99821	80	0.97182
30	0.99565	90	0.96535
40	0.99222	100	0.95840
50	0.98803		

The reciprocal of the density gives the specific volume of water at different temperatures. The change in specific volume of water with temperature is shown in Figure 8. As shown in the Figure 8, the volumetric behavior of water under temperature change is perfectly fitted with a fourth-order polynomial equation. The specific volume of water at any given temperature from 0°C to 100°C can be estimated by the regression equation shown in Figure 8. Now the volume change of water for any temperature change within the range of 0°C to 100°C can be obtained as:

$$\gamma_w = \frac{\Delta V}{V} \cdot \frac{1}{\Delta T} = \frac{W \cdot (v_2 - v_1)}{W \cdot v_1} \cdot \frac{1}{\Delta T} = \frac{v_2 - v_1}{v_1 \cdot (T_2 - T_1)} \qquad (6)$$

where V = initial volume of water,

ΔT = change of temperature from T_1 to T_2,

ΔV = change of volume of water due to the temperature change,

W = weight of water,

v_1 and v_2 = specific volumes of water at temperatures T_1 and T_2, respectively.
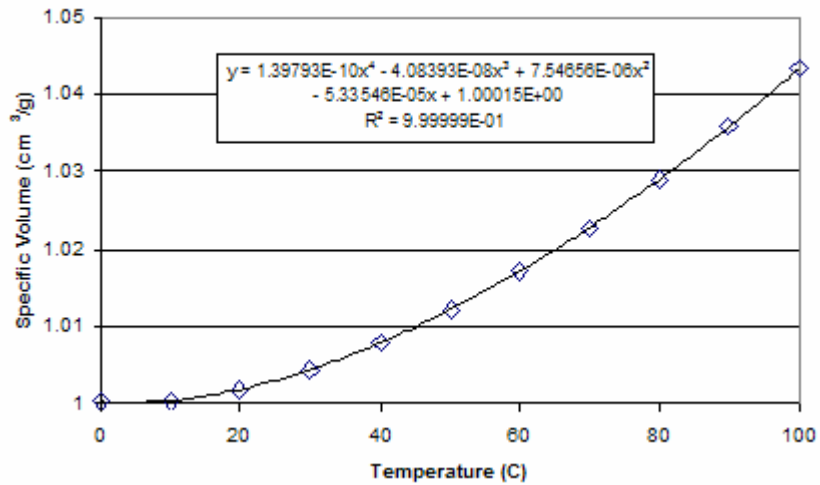
Figure 8 Thermal Expansion of Water.

Estimation of Errors

Random or systematic errors may exist in the test protocol. Error and sensitivity are evaluated with respect to the determination of input parameters and subsequent calculation of the CoTE of aggregate.

In determining the initial volume, it is assumed that the water level is always at the same position as long as the same graduation is used for the leveling. Precisely speaking, however, even if the same graduation is used, the level of water may vary slightly within the diameter due to the surface tension of the water. Consequent random error may exist in determining the initial total volume. Presumably, however, the effect of this error is not significant. The possible maximum error in CoTE caused by this random error in the water leveling process is less than ±1.0 percent. Furthermore, the actual error in the positioning the water would be much less than the maximum error level. Therefore, the possible random error in positioning the initial water level can be regarded as negligible as long as the same graduation is used for leveling the water.

Another random error may exist in determining the initial volume of aggregate associated with the measurements of the weight of aggregate. The effect of error in weight on the determination of volume is not significant. However, it should be recognized that the initial volume of aggregate could influence the determination of the aggregate CoTE, as previously noted. Considering that, in general, 3300 – 3700 g of saturated surface dry aggregate is used for a normal CoTE test, it is expected that the maximum random error in measuring the weight of aggregate would not be more than 5 g (0.125 percent). The thermal coefficient of the dilatometer is assumed to be a constant as long as the shape, size, and material of dilatometer remain same. If there is a difference between different dilatometers, maximum error expected in the coefficient of thermal expansion of flask (γf) is 1 percent. The sensitivity of the measurements on Δh is greater than other parameters. Considering that the general range of Δh is determined to be 15 to 20 mm, an error of only a few tenths of a millimeter produces significant error. This means the LVDT needs to be calibrated at least to 1/100 mm, which is in the range of its precision. It should be recognized that the thermal coefficient of water is much higher than the coefficient of the aggregate sample so the majority of the volumetric expansion is governed by water. Table 4 presents a summary of estimated factors of errors and their significance. Appendix C provides the details of variance analysis done on these factors.

Table 4 Possible Factors of Error and Their Significance.

Type	Factor	Coefficient of Variation of γ_a
Random	Positioning the initial water level	-
	Weight of aggregate	2.4 %
Systematic	Thermal coefficient of dilatometer (γ_f)	1.2 %
	Displacement reading (Δh)	3.9 %

Verification of the Test Method

As previously noted, measurement errors associated with temperature change, float displacement, and initial volume contribute to the error in determining the CoTE of aggregate. In order to develop a procedure to reduce the calculated error, a series of verification tests were conducted such as:

1. The test results from the dilatometer were compared with the results from strain gage setups for samples (steel and glass) with known CoTE values.

2. The repeatability of the dilatometer tests with the same aggregate sample was verified.

3. The data was tracked at a constant temperature condition to see if any systematic problems exist in the dilatometer test setup.

Tests for Steel and Glass Samples

The validity of the dilatometer tests was examined by comparing CoTE values obtained from the dilatometer with CoTE values from and different test schemes that use strain-gaged specimens. Two different materials, steel rods and glass rods, were used in these comparative tests. The steel and glass rods were specially prepared at 1 to 2 cm diameter and 12 cm length.

First, the comparison was made for steel rod test results. Figure 9 shows the results of two sets of tests using a strain gage method. Linear expansion of the steel bar was measured by the attached strain gage and relevant data logging device while temperature varies between T_1 and T_2. The tested temperature range was −13°C to 22°C. A separate thermocouple was attached to the surface of the steel rod to measure the actual steel temperature. As shown in Figure 9 thermal expansion of the steel rod was linear.

Therefore, the CoTE of the steel rod can be estimated as the slope of the best-fit line. The CoTE of steel rods was determined to be $11.24 \times 10^{-6}/°C$ with 3.2 percent covariance. As seen in table 5, the average CoTE of steel rods obtained from the dilatometer tests was $11.14 \times 10^{-6}/°C$ with 4.8 percent covariance. These two results support each other; the difference of the two results is less than 1 percent.

Table 5 shows the results of dilatometer tests for the steel rods. T_1, T_2, and Δh represent the measured initial and final temperatures and displacement of water, respectively. The actual temperature readings from the inside of the dilatometer are noted in table. Figure 10 shows actual data readings from test number 1 as a typical example of data measurements from the dilatometer.

For verification, the same comparative tests were conducted on glass rod samples. Table 6 shows the comparison of the results from the two different tests. The average CoTE of glass rods obtained by the two dilatometer tests is $8.27 \times 10^{-6}/°C$, and the difference between this and the strain gage test result is 1.8 percent. As presented, both steel and glass rod test results strongly support the reliability of the dilatometer test protocol.

Table 5 Dilatometer Test Results for the Steel Rod Samples.

Test No.	T_1 (°C)	T_2 (°C)	Δh (mm)	CoTE ($\times 10^{-6}/°C$)	Remark
1	10.38	50.33	14.573	11.54	Average: 11.13 St Dev.: 0.503
2	10.47	50.40	14.993	11.32	
3	10.50	50.41	14.809	10.58	

$CoTE = 11.24 \times 10^{-6}/°C$ Std dev = 0.36 R^2 =.983
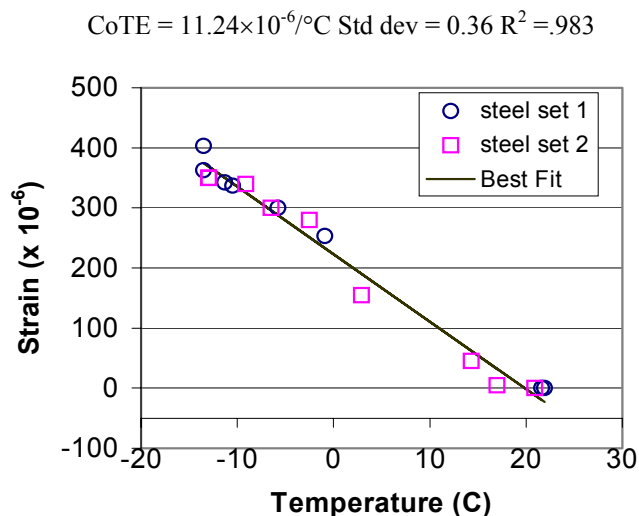
Figure 9 Thermal Expansions of Steel Rod Samples Measured by Strain Gage.

Based on these results, a correction of 0.2 percent to the change in float level should adequately calibrate and adjust the calculated CoTE, to the true value. This is an increase in CoTE since the calibration results were lower than the true results.

Repeatability of Dilatometer Tests in Measuring Aggregate CoTE

Repeatability of the dilatometer test protocol was investigated by repeating the test on a single aggregate sample. In fact, the verification tests described in the above section also indicated good repeatability. Each of the three tests on the steel samples as well as the latter two tests on the glass rods produced very similar CoTE values for each material set. In this section, the Abilene limestone sample was tested three times and the results were compared. Table 7 shows the comparisons of repeated test results.
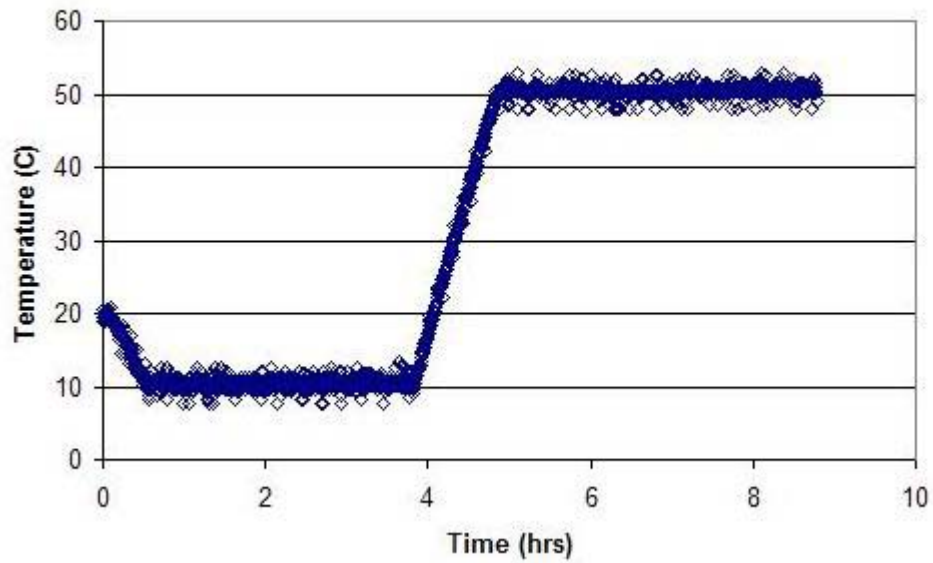
(a) Temperature measurements
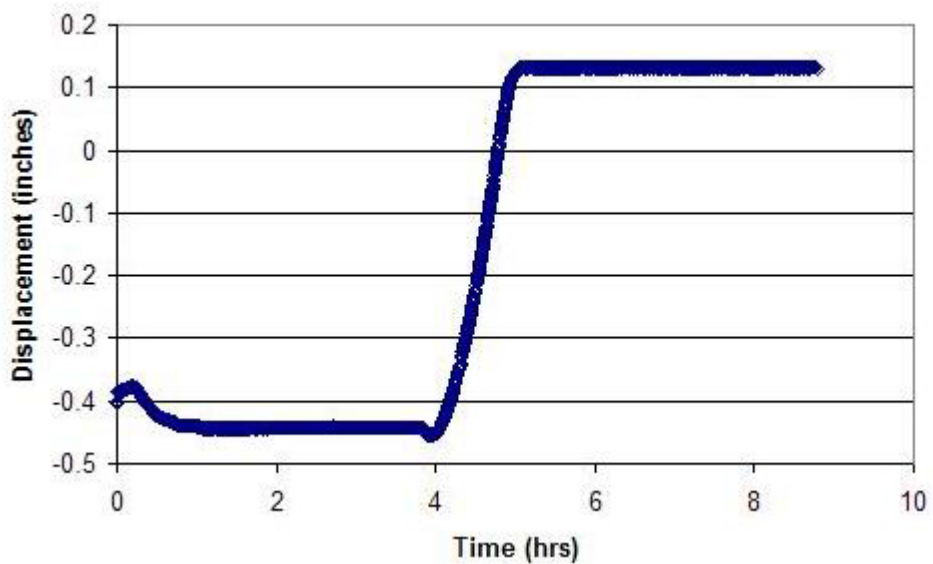
(b) Corresponding displacement of the water level at the tower of dilatometer

Figure 10 Typical Data Measurements of Dilatometer Tests.

Table 6 Comparison of CoTE of Glass Rods Obtained by Dilatometer and Strain Gage.

Test	T_1 (°C)	T_2 (°C)	CoTE ($\times 10^{-6}$/°C)
Dilatometer 1st	10.35	50.45	8.46
Dilatometer 2nd	10.28	50.31	8.08
Strain Gage	-13.6	21.3	8.42

Table 7 Comparison of Repeated CoTE Tests for Abilene Limestone.

Test	Initial sample weight (g)	Volume ratio (V_a/V)	T_1 (°C)	T_2 (°C)	Δh (mm)	CoTE ($\times 10^{-6}$/°C)
1	3967.2	0.4937	10.45	50.42	16.701	5.78
2	4054.4	0.5044	10.55	50.71	16.601	6.41
3	4054.4	0.5055	10.41	50.58	16.381	5.98

The initial sample weight is in SSD, condition and the volume ratio represents the ratio of initial volume of aggregate sample (V_a) to the initial total volume (V). The dilatometer was not opened between tests 2 and 3 and was left in the water bath until it cooled to room temperature so that the same sample was used for the last two tests. Note that the initial volumetric relations are different even for those two tests because the measured initial temperatures are different. Comparison of repeated test results indicated that the dilatometer produces acceptable repeatability. The average CoTE of the three tests is 6.05×10^{-6}/°C with 5 percent.

Tests at Constant Temperature Conditions

Possible systematic errors of the test system were investigated by testing under two different constant temperature conditions. In the first test, the dilatometer filled with water and aggregate sample was placed in the water bath, which was maintained at a temperature of 35°C. The data were collected as a normal CoTE test but longer period of time. The test result indicated that at least 2 hours of resting time was required after the final temperature was reached to get stable LVDT data. However, the maximum rebound of LVDT data is about 0.05 mm, from which the resulted error in CoTE is less than 2 percent. For a normal CoTE test, the displacement is averaged for at least 30 minutes data between 1.5 and 4 hours after the final temperature is reached. According to the trend of the LVDT data, the current data reduction method seems to be reasonable.

In the second test, the dilatometer was placed in the water bath at room temperature without operating the water bath and data were collected for 11 hours. The slight decrease in measured temperature is believed to be caused by the decrease of the room temperature during the night. The trend of the data shows (Figure 11) the conformity between test volume and temperature.
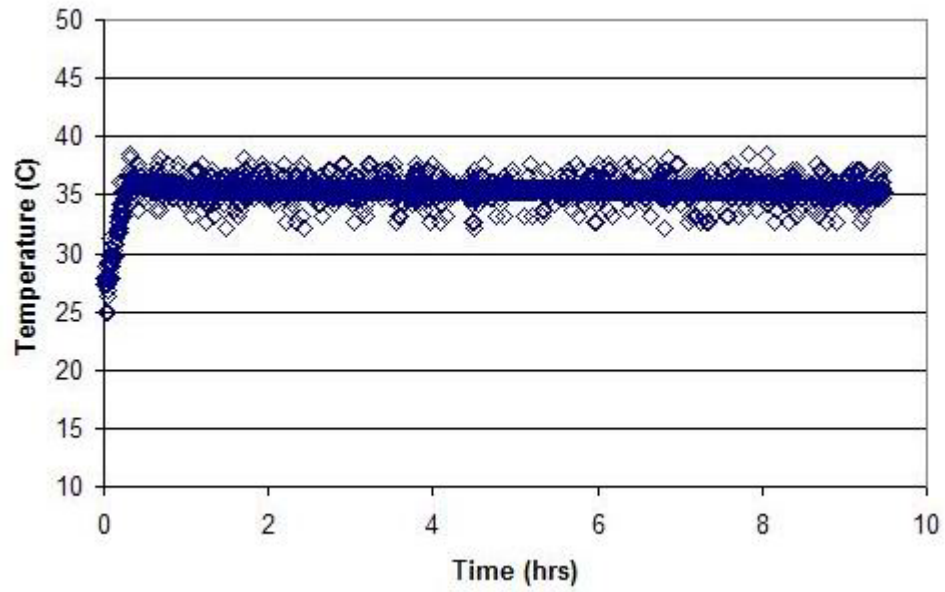
(a) Temperature measurements
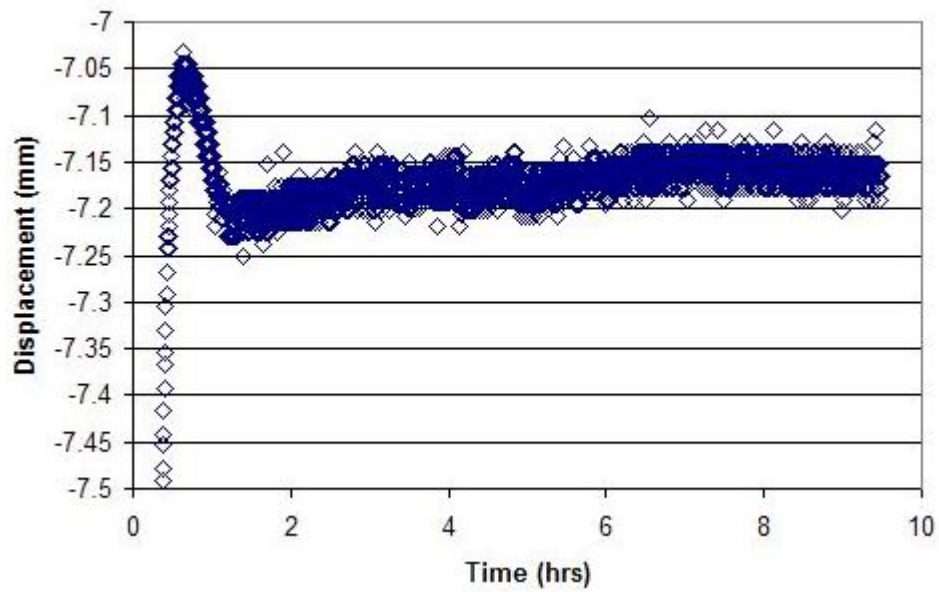
(b) Corresponding LVDT measurements

Figure 11 Data Collections at a Constant Temperature (35°C).

TESTING PROTOCOL

There are four steps in the volumetric dilatometer test:

      1.   preparing the sample,

      2.   vacuuming,

      3.   testing, and

      4.   analyzing the results.

Preparing the Sample

A representative aggregate sample, one and one-half times the required volume, is selected.
The sample is properly washed to remove dust and unwanted particles, and is then
submerged in water to for at least 24 hours before starting of the test. After the sample is
taken out of water it is washed once again before placing it inside the dilatometer. The SSD
and the submerged weight of aggregate are taken using the Rice specific gravity method.
The volume of aggregate, V_a, is calculated using the equation below:

$$V_a = v \cdot (W_{SSD} - W_{SUB}) \qquad (7)$$

where v = specific volume of water at the initial temperature,

      W_{SSD} = weight of aggregate sample in saturated surface dry condition,

      W_{SUB} = weight of aggregate sample submerged under water.

In equation (7), the temperature dependence of the aggregate volume is accounted by the
specific volume of water at the specific temperature. The weights are independent of
temperature.

      The whole dilatometer is then filled with aggregate sample. The lid of the
dilatometer is screwed tightly and it is then filled with water to a certain level marked on
the lid window.

Vacuuming

Vacuuming is performed based on the guidelines provided in Appendix D.

Testing

The water level is set to the fixed position after vacuuming. The dilatometer is then placed

into the 24°C water bath. The LVDT is placed on the float rod through the tower. The float

is placed properly on the water surface by rotating the LVDT and observing the change in

reading on the monitor. The reading of the LVDT is monitored for 15 minutes more to

make sure that there is no leak from the dilatometer. Then the water bath temperature is

adjusted to the initial temperature (T_1), i.e., 10°C. It takes around 0.5 hour to reach 10°C.

The temperature stabilizes at 10°C after 1.5 hours. The initial water temperature inside

dilatometer container and the position of the water surface (h_1) are automatically recorded

by the data acquisition system. Then the temperature is changed to final temperature (T_2),

i.e., 50°C. The position of the water surface at temperature T_2, denoted by h_2, is recorded by

the LVDT and the data acquisition system. Consequently, the rise of the water surface when

temperature is increased by ΔT from T_1 to T_2 is $\Delta h = h_2 - h_1$.

Analysis

The average coefficient of thermal expansion of the aggregate from T_1 to T_2 can be

calculated from V_a, V, Δh, ΔT, γ_w, and γ_f with equations (4) and (5), where $\gamma_f = 5.3 \times 10^{-5}$/°C. The dilatometer-measured CoTE values of the different types of aggregates are

presented in a later section.

4. MODELING APPROACH

INTRODUCTION

As already discussed in section 1 CoTE of the aggregate is mainly dependent on CoTE of the constituent minerals and their respective volume in aggregate. In this context, a new mineralogical approach to model aggregate CoTE has been introduced. Modeling of coefficient of thermal expansion will provide the person to predict the CoTE values based on the aggregate mineralogical contents and the mortar fraction in concrete. One can come up with different designs based on different ratios of constituents for concrete and steel if the specified CoTE value is met, without even doing much testing. This method reduces not only the effort and expenses on sample preparation of concrete and testing but the time also.

Since aggregates are composite material consisting of different minerals in different proportions, it is assumed that their properties can be determined from the properties of component minerals (*10*). A composite model to predict aggregate CoTE by using the CoTE of constituent minerals and their respective volume percentages has been introduced. Accuracy of the aggregate CoTE prediction by this composite modeling is mainly dependent on the accuracy of the CoTE of the individual pure minerals contained in the aggregates. Volumetric dilatometer testing method (*11*), which has been established earlier to measure aggregate and concrete CoTE (*21*), is used to accurately measure the CoTE of individual pure minerals. CoTE of individual aggregate is also estimated by dilatometry. Favorable comparison between the modeled and the measured aggregate CoTE provided a logical approach to establish a mineralogical composite model as a means to predict the aggregate CoTE. After determining the CoTE of aggregate, it is then attempted to predict the concrete CoTE based on the same principal of composite modeling in two component

system i.e. aggregate and mortar. Like aggregate CoTE, predicted concrete CoTE is also validated by drawing favorable comparison between predicted and measured concrete CoTE.

Basically, there are two models that predict the properties of a composite from those of its components: the parallel model and the series model. Constituent minerals in the aggregate are the components in the aggregate CoTE model, whereas mortar and coarse aggregate are the components in the concrete CoTE model. In the parallel model, the components of a composite are assumed to be combined in parallel. In the case of concrete, cement mortar and aggregate are the parallel components, as shown in Figure 12(a). When the concrete is loaded, mortar and aggregate are both displaced, so that the strain in both the components is same. The series model is illustrated in Figure 12(b), where the total displacement of the concrete under a tension force is the sum of the displacement of the constituent mortar and aggregate. The stress in the constituent mortar and aggregate is uniformly distributed. Hirsch's model (*10*) is a combination of the above two models and which has been used to predict the elastic modulus of concrete (Figure 12(c)). The present aggregate and concrete CoTE model is based on the concept of Hirsch's composite model.

The derived formulae for the aggregate and concrete CoTE models based on Hirsch's composite model are presented later.

MODELING OF AGGREGATE CoTE

A model is proposed to predict aggregate CoTE based on the calculated mineral weight percentages, measured pure mineral CoTE, and their modulus of elasticity (MOE). Minerals present and their respective weight percentages in the aggregates are calculated from the bulk chemistry (i.e., elemental oxide weight percentages of the aggregates). The CoTE of

common pure minerals was measured by dilatometry, and MOE of minerals were collected from literature. The prediction model for the aggregate CoTE is then formulated based on Hirsch's composite model (*10*).

Materials and Test Methods

Five different types of commonly used aggregates, namely, siliceous river gravel (SRG), calcareous river gravel (CRG, mainly calcareous with siliceous impurities), pure limestone, sandstone, and granite were collected from different areas across the state of Texas. CoTE was determined on samples of five pure minerals, namely, calcite, quartz, dolomite, albite (Na-feldspar), and microcline (K-feldspar) obtained from Ward's Natural Science Est. Inc. by dilatometry tests. These five minerals represent, to a large extent, the expected mineralogy of the above aggregates. The effect of other commonly occurring minor minerals (e.g., pyroxenes, magnetite/hematite, micas) on aggregate (e.g., granite) CoTE was assumed to be insignificant.
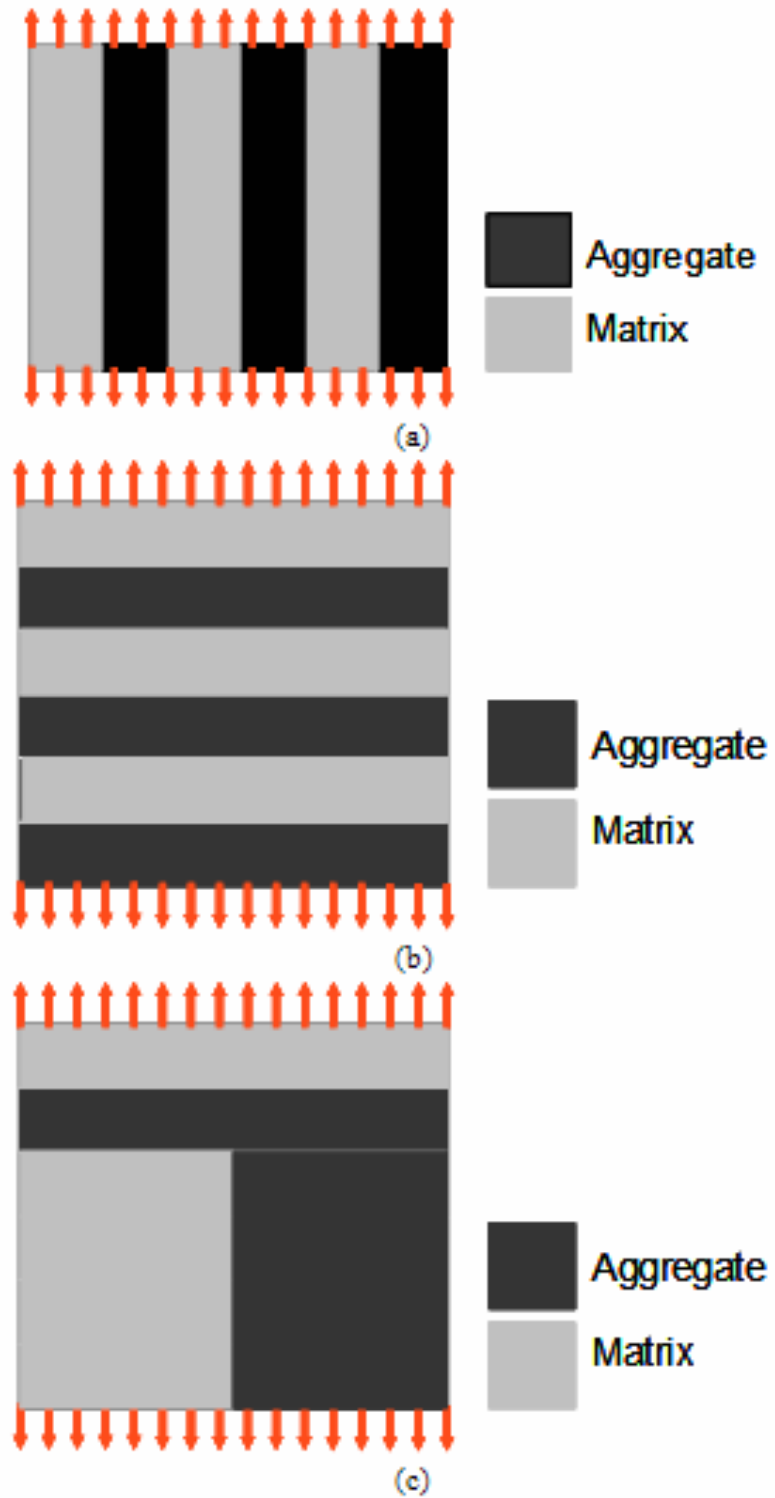
Figure 12 Composite Models for Concrete CoTE Calculation: (a) Parallel Model (b) Series Model (c) Hirsch's Model.

Bulk chemical analyses of representative powder samples of the above aggregates were carried out by X-ray fluorescence (XRF) at Wyoming Analytical Laboratories, Inc., located in Golden, Texas. Calculated mineralogy obtained by the proposed model (discussed later) for each aggregate was verified by X-ray diffraction (XRD, Rigaku Miniflex) at Texas Transportation Institute (TTI). Concrete cylinders of 8×4 inches were cast using the above-mentioned coarse aggregates, fine aggregate (single source), type I cement, and fly ash with 0.42 water/(cement + fly ash) ratio. A standard mortar using the same sand and maintaining the same ratio of sand:cementitious materials in concrete was cast. Dilatometry (*11*) was used to measure the CoTEs of the individual pure minerals, above-mentioned aggregates, mortar, and concrete. Cylindrical mortar and concrete specimens (5.6×4 inch) were obtained from the original 8×4 inch specimens, and measurement of CoTE by dilatometer was performed after 28 days of moist curing. Representative samples from as-received loose aggregate were prepared following the protocol explained in Appendix E and used to measure aggregate CoTE.

Elemental oxide weight percentages for all prepared aggregate powder samples were determined by XRF and are presented in Table 8.

Determination of Mineral Weight Percentages from Bulk Chemical Analysis
As previously noted, minerals present in an aggregate source and their respective weight percentages can be estimated from the elemental oxides as determined by chemical analyses. Two different schemes of calculation were proposed to determine mineral weight percentages from bulk chemical analysis of aggregate. This calculation represents a wide range of rocks (i.e., sedimentary, igneous, and their metamorphic equivalents) commonly

used as aggregates and provides a realistic representation of the mineral phases present in

different types of aggregate.

Table 8 Bulk Chemical Analyses of the Tested Aggregates.

Aggregate	Sample No.	Bulk chemical analyses (wt%)							
		SiO_2	Al_2O_3	Fe_2O_3	CaO	MgO	Na_2O	K_2O	LOI
Gravel (siliceous) SRG	1	94.17	0.93	0.94	1.78	0.00	0.22	0.28	1.68
	2	96.86	0.79	1.01	0.54	0.11	0.00	0.14	0.55
Gravel* (calcareous), CRG	3	35.57	1.20	2.30	32.20	1.50	0.00	0.30	26.46
	4	22.13	0.29	2.72	40.31	1.39	0.00	0.24	32.67
Limestone (Lst)	5	2.28	0.47	0.24	53.76	0.52	0.00	0.05	42.53
	6	0.26	0.11	0.04	55.33	0.39	0.01	0.01	43.73
	7	2.57	0.24	0.65	53.07	0.61	0.00	0.07	42.39
	8	5.97	0.23	0.86	51.07	0.86	0.00	0.07	40.92
	9	6.21	0.11	0.06	51.53	0.86	0.05	0.01	41.17
	10	0.34	0.00	0.08	54.16	1.67	0.08	0.02	43.65
	11	0.24	0.00	0.03	56.16	0.15	0.00	0.00	43.42
Sandstone (Sst)	12	79.84	8.43	4.51	1.09	0.845	1.43	1.95	1.67
	13	90.16	2.70	3.28	0.62	0.22	0.30	0.58	2.13
Granite	14	72.14	13.62	3.28	1.24	0.28	3.86	4.92	0.02
	15	68.97	13.45	5.21	2.18	0.80	3.72	4.23	0.21

*Mainly calcareous with siliceous impurity.

Method I

This method was used to calculate weight percentages of seven minerals (dolomite,

albite, orthoclase, anorthite, quartz, calcite, and magnetite) and is applicable to aggregates

belonging to the sedimentary group of rocks and their metamorphic equivalents (e.g.,

limestone, gravel, sandstone, marble, etc). These seven minerals cover the major

constituents in most sedimentary rocks and their metamorphic equivalents, which are

commonly used as aggregates. This calculation method is based on an allotment of

elemental oxide weight percentages to mineral weight percentages according to

stoichiometric chemical equations for minerals (Appendix F). This method is not used for

shale, siltstone, or schist rocks because of limitations in calculating the micaceous and clay

minerals. However, the practice of using these types of rocks as concrete aggregate is somewhat limited. The following assumptions were considered for simplification of the calculation (Appendix F):

- All SiO_2 is allocated to quartz and feldspar. The three most commonly occurring types of feldspar (i.e., potassium feldspar [orthoclase/microcline], sodic-feldspar [albite] and calcium feldspar [anorthite] are considered for the calculation.

- All CaO is allocated to calcite, dolomite (to combine all MgO), and anorthite (to combine, if any, leftover Al_2O_3 after orthoclase and albite).

- All Fe_2O_3 is allocated to magnetite or hematite because chemical analysis generally includes all Fe in Fe_2O_3 or FeO.

Method II

This method is used to calculate weight percentages of nine minerals (apatite, ilmenite, orthoclase, albite, anorthite, pyroxenes, olivine, quartz, and magnetite/hematite) and is applicable to aggregates belonging to the igneous suite of rocks and their metamorphic equivalents (e.g., granite, basalt, granulites, and ultrabasic rocks, etc). Method I cannot be used to calculate the mineralogy of these rocks because:

1. The allotment of SiO_2 only to feldspars and quartz (method I) is not valid for these rock types. Ferromagnesian silicates (e.g., pyroxene, olivine) are essential mineral phases in these suites of rocks and they also contain SiO_2. Ultrabasic rocks do not contain quartz, which can only be reflected by method II.

2. Calcite and dolomite are not present in the igneous suite of rocks as a primary crystallizing phase. Therefore, allotment of CaO to calcite and dolomite is not valid

for these groups of rocks where the primary source of CaO is Ca feldspar (anorthite) with minor contributions from pyroxenes (e.g. diopside) and amphiboles.

The calculation of method II is based on proper sequential allotment of the molecular proportion of elements to mineral weight percentages based on the crystallization sequence in magma. Detailed steps for the calculation of method II are presented in Appendix F.

The following selection criteria were followed based on bulk chemical analysis to determine the suitable method for the sampled aggregate:

- $SiO_2 \geq 80$ percent (e.g., sandstone, fine sand aggregates, siliceous gravel, metaquartzite, etc.) - Method I
- $CaO \geq 30$ percent and LOI ≥ 25 percent (e.g., limestone, marble, etc.) - Method I
- $SiO_2 = 38\text{-}75$ percent, $Al_2O_3 = 10\text{-}18$ percent and $CaO < 20$ percent (igneous rocks, e.g., granite, rhyolite, andesite, diorite, basalt, gabbro, etc.) - Method II

The proposed methods were applied to calculate mineral weight percentages from bulk chemical analysis of the respective aggregate powder samples and are presented in Table 9. Table 9 also shows the presence of actual minerals identified by XRD. A perusal of Table 9 shows that calculated mineralogy based on the proposed method closely resembles with the actual mineralogy identified by XRD. This supports the capability of the proposed method to calculate the mineralogy in a more realistic manner.

Table 9 Calculated Mineral Volume (Percent) by the Proposed Methods for the Tested Aggregates along with Actual Minerals Identified by XRD for Some Selected Aggregates.

Aggregate	Samp. No.	Mineral volume (%)								Minerals identified from XRD
		Do	Cc	Ab	An	Pf	Qtz	Mt	Pyx	
SRG METHOD I	1	0.00	2.73	1.91	0.69	1.71	92.25	0.69	0.00	Qtz
	2	0.47	0.06	0.00	1.69	0.85	96.18	0.75	0.00	
CRG METHOD I	3	6.71	51.92	0.00	2.44	1.90	35.23	1.79	0.00	
	4	6.27	67.50	0.00	0.01	1.37	20.87	3.88	0.00	Cc, Qtz, Ab (t), Do (t)
Limestone METHOD I	5	2.37	94.23	0.00	1.17	0.32	1.71	0.19	0.00	
	6	1.77	97.73	0.09	0.24	0.06	0.07	0.03	0.00	Cc, Ab (t), Do (t)
	7	2.80	93.29	0.00	0.45	0.41	2.11	0.94	0.00	
	8	3.92	88.58	0.00	0.44	0.45	5.92	0.68	0.00	
	9	3.90	89.22	0.46	0.05	0.06	6.26	0.05	0.00	
	10	7.57	91.96	0.73	0.00	0.13	0.00	0.06	0.00	Cc, Ab (t), Do (t)
	11	0.68	99.04	0.00	0.00	0.00	0.26	0.02	0.00	
Sandstone METHOD I	12	3.56	0.00	12.13	10.46	11.60	58.95	3.31	0.00	
	13	0.96	0.00	2.66	4.29	3.61	86.93	2.51	0.00	
Granite, METHOD II	14	0.00	0.00	32.66	5.31	29.08	24.85	0.00	6.29	Qtz, Ab, Pf, Pyx, Biotite, Muscovite
	15	0.00	0.00	31.48	7.50	25.00	22.33	0.00	11.31	

D – Dolomite, Cc – Calcite, Ab – Albite (Na-feldspar), Pf – K-feldspar, Qtz – Quartz, Mt – Magnetite, Pyx – Pyroxene; t – trace amount

CoTE of Pure Minerals

The CoTEs of five natural pure minerals (calcite, dolomite, albite, orthoclase, and quartz) were measured by dilatometer and are presented in Table 10. These five pure minerals constitute the majority of expected mineralogy of the tested aggregates. The cylindrical 5.6 × 4 inch specimens were obtained from the bigger sized mineral specimens by coring and were used to measure CoTE in the dilatometer. Calcite, dolomite, and quartz were polycrystalline type, whereas albite and orthoclase were selected from cleaved blocks. Powder samples of the all the collected minerals were prepared and analyzed by XRD to check their purity. The minor phases identified as impurities are also listed in Table 11. Note that the minerals in natural aggregates also contain similar types of impurities. Therefore, the measured CoTE of these naturally occurring minerals with traces of impurities provides a more realistic mineral CoTE input for the aggregate CoTE modeling.

Composite Modeling to Predict Aggregate CoTE

The model to predict aggregate CoTE is based on the concept of Hirsch's composite model (*10*), where determined CoTE of pure minerals and their respective volume percent are the two main inputs. The following formula is derived based on Hirsch's composite modeling to predict aggregate CoTE:

$$\alpha_a = x\sum \alpha_i V_i + (1-x)\left\{\frac{\sum \alpha_i V_i E_i}{\sum V_i E_i}\right\} \qquad (8)$$

where α_a = CoTE of aggregate,

α_i = CoTE of individual mineral,

V_i = volume fraction of each mineral in aggregate, and

E_i = Young's modulus of each mineral phase.

X= relative proportions of material conforming with the upper and lower bound

solution.

Hirsch's model becomes the series model when X = 0, and it becomes the parallel

model when X = 1. A value of 0.5 is assumed for X and indicates that the chance of

occurrence of either parallel or series arrangements of the constituent minerals in the

aggregate is equal. The predicted aggregate CoTE based on CoTE and elastic modulus of

pure minerals (Table 11) (*22*) and their respective calculated mineral volume percent are

presented in Table 12. The CoTEs of all the sampled aggregates were measured by

dilatometer and are also listed in the same table for comparison. Figure 13 shows the

graphical representation of measured vs. calculated CoTE of aggregates.

**Table 10 Comparative Assessments between Mineral CoTE (Linear) Measured by
Dilatometer and Collected from Literature.**

Mineral	Dilatometer	ASTM STP 169C	Handbook (*22*)
Dolomite	9.62	-	9.40*
Calcite	5.58	5.0	5.05*
Albite	6.52	6.0	6.00*
Anorthite	-	3.0	4.70+
Microcline	6.50	6.5-7.5	5.20+
Quartz	13.00	12.0	-
Magnetite	-	-	6.86+
Pyroxene	-	6.5 – 7.5	12.11*

*Average of 3 linear CoTE along three crystallographic direction (a,b,c)
  of single crystal; + linear CoTE = volume CoTE / 3

Table 11 CoTE of the Pure Minerals Measured by Dilatometer, Their Respective Elastic Modulus and Phases Identified as Impurities by XRD.

Minerals	CoTE measured (10^{-6}/°C)	CoTE from literature (*22*) (10^{-6}/°C)	Elastic modulus ($\times 10^6$ psi) (*22*)	Traces of minerals identified as impurity by XRD
Calcite	5.58		20.42	No impurity
Dolomite	9.62		29.07	1.Ankerite [Ca(Fe,Mg)(CO$_3$)] 2.Minrecordite [CaZn(CO$_3$)]
Quartz	13.00		12.30	No impurity
Microcline	6.60		9.50	Disordered albite (NaAlSi$_3$O$_8$)
Albite	6.80		10.50	Anorthite (CaAl$_2$Si$_2$O$_8$)
Anorthite		4.70	17.60	Albite (NaAlSi$_3$O$_8$)
Magnetite	—	6.86	38.30	
Pyroxene	—	12.11	32.50	

Table 12 Mineral Volumes (Percent) and Calculated CoTE for the Tested Aggregates along with Measured CoTE by Dilatometer.

Aggregate	Sample No.	Mineral volume (%)								CoTE (10^{-6}/°C)	
		Do	Cc	Ab	An	Pf	Qtz	Mt	Pyx	Cal.	Msd.
SRG Method I	1	0.00	2.73	1.91	0.69	1.71	92.25	0.69	0.00	12.39	12.30
	2	0.47	0.06	0.00	1.69	0.85	96.18	0.75	0.00	12.70	13.10
CRG Method I	3	6.71	51.92	0.00	2.44	1.90	35.23	1.79	0.00	8.20	9.19
	4	6.27	67.50	0.00	0.01	1.37	20.87	3.88	0.00	7.23	
Limestone Method I	5	2.37	94.23	0.00	1.17	0.32	1.71	0.19	0.00	5.81	6.35
	6	1.77	97.73	0.09	0.24	0.06	0.07	0.03	0.00	5.67	6.74
	7	2.80	93.29	0.00	0.45	0.41	2.11	0.94	0.00	5.87	6.27
	8	3.92	88.58	0.00	0.44	0.45	5.92	0.68	0.00	6.14	
	9	3.90	89.22	0.46	0.05	0.06	6.26	0.05	0.00	6.15	6.45
	10	7.57	91.96	0.73	0.00	0.13	0.00	0.06	0.00	5.96	
	11	0.68	99.04	0.00	0.00	0.00	0.26	0.02	0.00	5.63	
Sandstone Method I	12	3.56	0.00	12.13	10.46	11.60	58.95	3.31	0.00	10.35	10.30
	13	0.96	0.00	2.66	04.29	3.61	86.93	2.51	0.00	12.05	12.00
Granite, Method II	14	0.00	0.00	32.66	5.31	29.08	24.85	0.00	6.29	8.93	8.81
	15	0.00	0.00	31.48	7.50	25.00	22.33	0.00	11.31	9.28	9.00

Cal. – Calculated, Msd. – measured; Do – Dolomite, Cc – Calcite, Ab – Albite (Na-feldspar), Pf – K-feldspar, Qtz – Quartz, Mt – Magnetite, Pyz – Pyroxene

Perusal of Figure 13 shows that the predicted CoTE by modeling closely resembles the measured CoTE as is evident from higher correlation coefficients (0.98) between calculated and measured CoTE. Calcareous gravel (impure limestone) deviates slightly from the main trend. Calcareous gravels show slightly higher measured CoTE (9.19×10^{-6}/°C) than the predicted CoTE (8.2×10^{-6}/°C). However, additional testing of other calcareous gravels needs to be performed in order to verify whether this type of aggregate always shows slightly higher measured than predicted CoTE.

Aggregate source variability should be reflected in variations in elemental oxide weight percentages if properly sampled. Variation in elemental oxide weight percentages results in mineralogy changes and, hence changes in CoTE. As, for example, the CoTE of pure limestone is 5.7- 6.2×10^{-6}/°C, whereas, that of impure siliceous limestone is give 7.2- 8.2×10^{-6}/°C. Therefore, the present mineralogical modeling approach is a sensitive tool to monitor the aggregate source variability and has great potential for aggregate quality control.
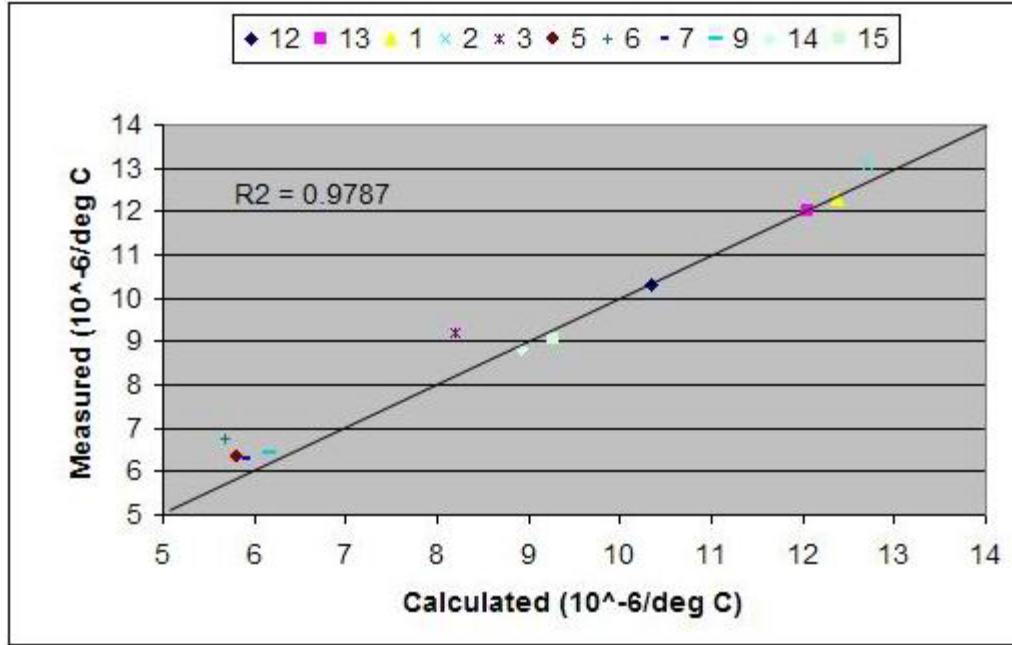
Figure 13 Calculated vs Measured Aggregate CoTE.

MODELING OF CONCRETE COTE

The model to predict concrete CoTE is based on the concept of Hirsch's composite model, where determined CoTEs of mortar and coarse aggregate are the two main inputs. Our proposed concrete CoTE model is basically a two-step model (i.e., (i) prediction and validation of aggregate CoTE, elaborated in the foregoing discussion, and (ii) prediction of concrete CoTE based on calculated CoTE of aggregate in the first step (Table 12) and known CoTE of standard mortar). Measured concrete CoTE by dilatometer validates the concrete CoTE model by comparing the predicted value to the measured value. The following formula is derived based on Hirsch's composite modeling to predict concrete CoTE:

$$\alpha_c = X(\alpha_m V_m + \alpha_a V_a) + (1 - X)\frac{\alpha_m V_m E_m + \alpha_a V_a E_a}{V_m E_m + V_a E_a} \tag{9}$$

where α_m, α_a = CoTE of mortar and aggregate,

V_m, V_a = volume fraction of mortar and aggregate,

E_m, E_a = elastic modulus of mortar and aggregate, and

X = relative proportions of material conforming with the upper and lower bound solution.

The CoTE of a standard mortar specimen (14.5×10^{-6}/°C) using the same sand and similar sand: cement ratio that was used in the concrete was measured by dilatometer and used as the fixed-mortar CoTE input in the concrete CoTE model. Volume fractions of mortar and aggregate are calculated from mixture proportions of the tested concrete specimens and are given in Table 13. A value of 1×10^6 psi was used as the fixed input for MOE of mortar. It is observed that MOEs of $5\text{-}10 \times 10^6$ psi represent nearly all natural rocks commonly used as aggregates. Research have found from modeling of elastic modulus that, at least for some concretes, X is approximately 0.5 (*23*). Therefore, 0.5 was assigned for X in the present study.

Cast concrete specimens (cylindrical 8×4 specimens) were sliced into 4 (diameter) $\times$ 5.5 (height) inch dimensions after 28 days of moist curing. The CoTE of these sliced cylindrical specimens was measured by dilatometer after curing them in 100 percent humidity chamber for 28 days. Predicted and measured concrete CoTEs are presented in Figure 14. Perusal of figure indicates that predicted CoTE shows good correlation with measured CoTE, with correlation coefficient of around 0.97. The effect of changing aggregate MOE (from 5×10^6 to 10×10^6 psi) on predicted concrete CoTE was also checked. It was observed that the predicted concrete CoTE slightly decreases with increasing aggregate MOE. It is interesting to note that the correlation coefficient between predicted and measured CoTE remains unchanged while changing aggregate MOE.

Therefore, a fixed value of 8×10^6 psi as aggregate MOE is considered in the present study to predict concrete CoTE for simplicity. However, one can use the actual elastic modulus of tested aggregate to predict the concrete CoTE.

Table 13 Mix Proportions of Concrete Specimens.

Type of coarse aggregate	Coarse aggregate (kg)	Fine aggregate (kg)	Cement (kg)	Fly ash (kg)	Water (kg)	Ap. SG (CA)	V_{CA}	V_m
SRG-1	1050	636.54	273	117	163.8	2.62	0.4214	0.5786
SRG-2	1050	628.56	273	117	163.8	2.60	0.4247	0.5753
CRG-3	1050	632.57	273	117	163.8	2.61	0.4230	0.5769
Lst-5	1050	636.54	273	117	163.8	2.62	0.4214	0.5786
Lst-6	1050	636.54	273	117	163.8	2.61	0.4223	0.5776
Lst-9	1050	632.57	273	117	163.8	2.60	0.4240	0.5760
Sst-12	1050	659.77	273	117	163.8	2.67	0.4128	0.5872
Granite-14	1050	652.14	273	117	163.8	2.65	0.4150	0.5850
Granite-15	1050	652.14	273	117	163.8	2.66	0.4150	0.5850

CA – Coarse aggregate, SG – Specific gravity, V_{CA} – Volume fraction of CA, V_m – Volume fraction of mortar, Lst – Limestone, Sst – Sandstone; Type of coarse aggregate is in accordance with Table 13.
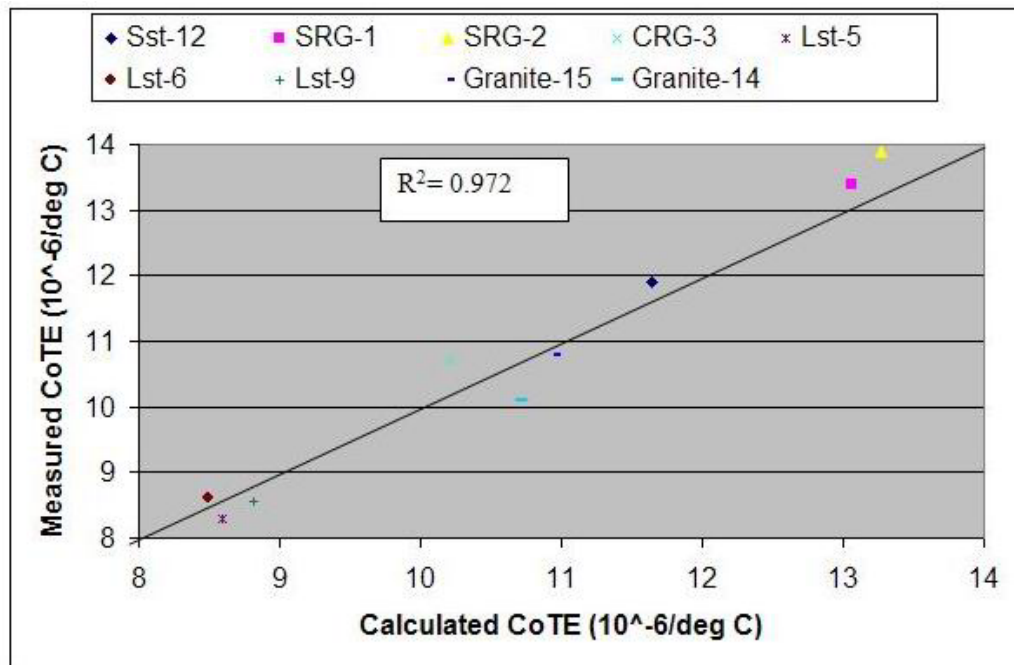

Figure 14 Calculated vs. Measured Concrete CoTE where X = 0.5 and MOE for Coarse Aggregate = 8×10^6 psi.

5. SUMMARY AND CONCLUSION

This report discussed the volumetric dilatometer test method to measure aggregate and concrete CoTE. The new approach to predicting the aggregate and concrete CoTE based on the mineralogy of the aggregate and the mix proportions of the concrete is also well elaborated.

Under a change in temperature, an unrestrained material will change shape proportional to the amount of temperature change multiplied by its coefficient of thermal expansion. The CoTE indicates how much material shape will change for each degree of temperature change. The CoTE is, therefore, a fundamental engineering property that quantifies the change in unit length per degree of temperature change. This will be a factor to determine the type of aggregate can be used to keep the crack of a concrete pavement to a maximum specified width because crack width is one factor which determines the load transfer efficiency of concrete pavements.

As aggregates themselves comprise of a variety of minerals, it has been shown that their CoTE varies with mineralogical composition and porosity. Quartz has the highest CoTE of any common mineral, and aggregates with high quartz content have high CoTE values. The CoTE of hardened concrete is variable, depending on the mixture design and the type of aggregate used. Since aggregates make up the bulk of concrete, their properties will largely determine concrete's CoTE. With a known mixture proportion, the CoTE of hardened concrete can be estimated from a weighted average of all its components.

CONCLUSION

A new mineralogical approach is presented to predict aggregate and concrete coefficient of thermal expansion based on Hirsch's composite modeling. The following points are drawn as conclusions from the present study:

- The sampling protocol for the aggregate provides a consistent means to select a representative powder sample for bulk chemical analysis. However, more care should be taken for sampling gravel (especially calcareous gravel) aggregate.

- All three types of rocks (e.g., sedimentary, igneous, and metamorphic) commonly used as aggregates can be considered in the present model by maintaining their separate entity.

- Different aggregates are well represented by the weight percentage of minerals actually present. The calculated mineralogy based on the proposed modeling and actual mineralogy from XRD compare well. This similarity suggests that the combination of the proposed two methods is capable of calculating representative mineralogy for all types of aggregates.

- Dilatometer CoTE measurement of five pure minerals is fundamental to the development of a model for the prediction of aggregate CoTE. More accurate estimation of a pure mineral's CoTE leads to more accurate the better will be the prediction because individual mineral CoTE is the most important input when calculating aggregate CoTE.

- Predicted aggregate CoTE by mineralogical modeling compares well with the measured aggregate CoTE, except for with some minor deviation in calcareous gravel. This similarity validates the composite model for prediction of aggregate

CoTE. However, more research on different types of aggregates is needed to establish this resemblance, and hence, the effectiveness of composite mineralogical modeling to predict aggregate CoTE.

- Different aggregates contain different types of minerals, and this is well reflected in the proposed model. This difference in mineralogy gives rise to different CoTEs. Therefore, present mineralogical modeling is sensitive to categorizing aggregates based on their CoTE values.

- Predicted concrete CoTE by composite modeling and measured concrete CoTE by dilatometer shows good correlation. This correlation validates the effectiveness of composite modeling to predict concrete CoTE. A change of aggregate MOE from 5 $\times 10^6$ psi to 10×10^6 psi does not result in significant variation in concrete CoTE. Therefore, the composite model for prediction of concrete CoTE can be applied to concrete containing a wide variety of aggregates with different CoTEs and MOEs. Composite modeling will be useful as a check of aggregate source variability in terms of quality control measures and improved design and quality control measures of concrete. Further research needs to be done to test porous aggregates using dilatometer device.

The overall strategy to implement the measurement and specification of CoTE is shown in Figure 15 are divided into two main sections
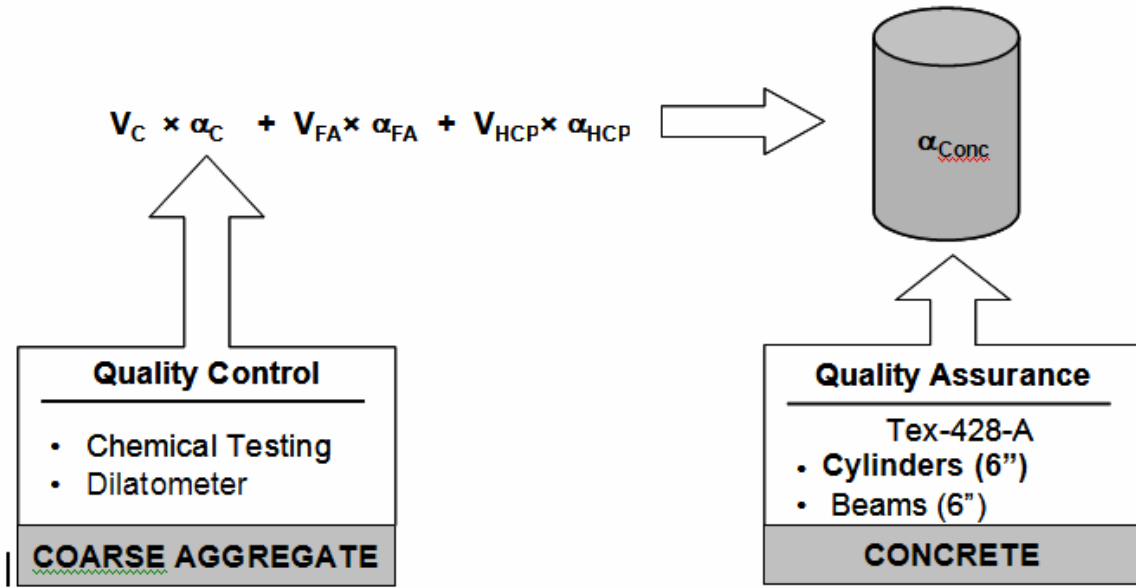
Figure 15 Schematic of Overall CoTE Implementation Strategy.

QUALITY CONTROL (QC) TESTING ON THE AGGREGATE SOURCE

In concept, coarse aggregates taken from various sources can be sampled at specified

intervals. After chemical analysis of the mineral composition of the aggregates, the

coefficient of thermal expansion of coarse aggregates (α_{CA}) can be predicted from results of

chemical or dilatometer testing. The aggregate coefficient of expansion (α_{CA}) is used along

with the concrete mixture proportions to calculate the CoTE of the concrete. As shown in

Figure 15, the CoTE of the concrete mixture (α_{Conc}) is then estimated based on a weighted

average of all the mixture components, which include the coarse aggregate (CA), fine

aggregate (FA), and the hydrated cement paste (HCP).

QUALITY ASSURANCE (QA) TESTING ON THE CONCRETE

During construction, QA testing on the concrete will be performed at specified intervals.

The specimens for this test will involve either the concrete as delivered to site (cylinders or

beams) or the concrete as placed (cores). Long-term pavement performance is related to the

in-situ CoTE value achieved, and enforcement could, therefore, eventually be based the percentage of design life that will result due to the CoTE as constructed.

SPECIFICATION DEVELOPMENT

Development of a draft specification (Appendix G) will provide guidelines for CoTE that ensure that design conditions are achieved during construction. The variability of aggregates and concrete CoTE values need to be addressed as part of the specification as well as aggregate prequalification, quality control testing, and quality assurance testing during actual construction.

The CoTE implementation approach for the QC and QA testing phases were previously shown in Figure 15. Quality control testing on the raw aggregate sources would eliminate the need for concrete samples. Quality control testing can either be based on chemical testing of the aggregate mineralogy or on dilatometer results. The required sampling procedure and frequency of testing are explained in Section 4.

Quality assurance testing should be performed on the hardened concrete. This is necessary to validate that the CoTE of the concrete as constructed meets the CoTE assumed during design. The dilatometer is recommended to determine the CoTE of concrete specimens. Ideally, the CoTE from samples cored out of the pavement should be tested, but it can also be determine, from molded specimens collected onsite. Six inch cylinders can be used for this purpose, but this would require that additional CoTE specimens be made. The other possibility is that 6 inch beams, commonly used for strength testing, be used for quality assurance testing. The frequency of quality assurance testing will also be addressed in the specifications.

CLASSIFICATION OF AGGREGATES BASED ON TEXTURE AND CoTE

The classification of the coarse aggregate can be done in a format of Tα-N where

- T represents the measure of aggregate texture that ranges from 0 to 1200, e.g., L –
  Low texture (<400), M – Medium texture (400-800), H – High texture (>800)
- α represents the measured CoTE of the aggregate in whole number of micro strain
  /°C with a range of 5 to 12 (2.78 to 6.66 micro strain /°F), e.g., L – low, M- Medium
  and H- High (refer Table 2).
- N represents name of the aggregate, e.g., siliceous river gravel (SRG), calcareous
  river gravel (CRG), limestone (LST), sandstone (SST), Granite (GRN)

A perusal of Table 14 below illustrates the aggregate classification system in the above
Tα -N format

Table 14 Aggregate Classification System in Tα -N Format

Texture (T)	CoTE (α)	Aggregate name (N)	Classification in Tα -N format
Low texture (L)	High (H)	SRG-uncrushed	LH-SRGUC
Low texture (L)	High (H)	SRG-crushed (e.g. chert dominated gravel)	LH-SRGC
Medium texture (M)	High (H)	SRG-crushed (quartzite dominated gravel)	MH-SRGC
Medium texture (M)	Low (L)	Limestone - LST	ML-LST
Low texture (L)	Low (L)	Limestone - LST	LL-LST
Medium texture (M)	Medium (M)	Siliceous limestone - SLST	MM-SLST
Medium texture (M)	Low (L)	Marble (MRB)	ML-MRB
Low texture (L)	Medium (M)	CRG-uncrushed	LM-CRGUC
Medium texture (M)	Medium (M)	CRG-crushed	MM-CRGUC
High texture (H)	Medium (M)	Granite - GRN	HM-GRN
Low texture (M)	Medium (M)	Basalt - BST	LM-BST
Medium texture (M)	High (H)	Sandstone - SST	MH-SST

Aggregate CoTE is classified in three categories based on their affect on concrete

pavements. Low CoTE value of aggregate is desired for better performance of pavements.

REFERENCES

1. McCullough, B. F., D. G. Zollinger, and T. Dossey. *Evaluation of the Performance of Pavements Made with Different Coarse Aggregates*. Research Report 3925-1F. Center for Transportation Research, The University of Texas at Austin, September 1998.

2. Mitchell, L. J. Thermal Expansion Tests on Aggregates, Neat Cements, and Concrete. *ACI Journal*, Vol. 48, June 1953, pp. 964-977.

3. Meyers, S. L. How Temperature and Moisture Changes May Affect Durability of Concrete. *Rock Products*, Vol. 54, No. 8, August, 1951, pp. 153-162.

4. Huang, Y. H. *Pavement Analysis and Design*. Prentice Hall, Englewood, New Jersey, 1993.

5. Neville, A. M. *Properties of Concrete*. John Wiley and Sons, New York, New, 1997.

6. Brown, R. D. *Thermal Movement of Concrete*. Current Practice Sheet, No. 3PC/06/01, Cement and Concrete Association, Wexham Springs, Slough, England, November 1972.

7. Won, M., K. Hankins, and B. F. McCullough. *Mechanistic Analysis of Continuously Reinforced Concrete Pavements Considering Material Characteristics, Variability, and Fatigue.* Report No. 1169-2, Center for Transportation Research, The University of Texas at Austin, April 1990.

8. Davis, R. E. A Summary of the Results of Investigations Having to Do with Volumetric Changes in Cements, Mortars and Concrete, due to Causes Other Than Stress. *ACI Journal*, Proceedings 26, June 1930, pp. 407- 443.

9. Mullen, W. G., D. L. Bloem, and S. Walker. Effects of Temperature Changes on Concrete as Influenced by Aggregates. *ACI Journal*, Vol. 48, April 1952, pp. 661-679.

10. Hirsch, T. J. Modulus of Elasticity of Concrete Affected by Elastic Moduli of Cement Paste Matrix and Aggregate. *ACI Journal*, Vol. 59, No. 3, March 1962, pp. 427-451.

11. Zollinger, D. G., T. Tianxi, D. Fowler, and L. Wang. *Development of a Test Apparatus to Measure Thermal Expansion of Concrete Aggregates*. Unpublishd Research Report (2992-1), Texas Transportation Institute, Texas A&M University System, College Station, 1998.

12. Willis, T. F., and M. E. DeReus. Thermal Volume Change and Elasticity of Aggregates and Their Effect on Concrete. *Proceedings, American Society for Testing and Materials,* Vol. 39 pp. 919- 928.

13. Corps of Engineers, U. S. Army. *Handbook for Concrete and Cement*. Complete Edition, Waterways Experiment Station, Vicksburg, Mississippi, August 1949.

14. Venecanin, S. D. Thermal Incompatibility of Concrete Components and Thermal Properties of Carbonate Rocks. *ACI Materials Journal*, Vol. 87, 1990, pp. 602-607.

15. Mitchell, L. J. Thermal Expansion Test on Aggregate, Neat Cement and Concrete. Proceedings, *American Society for Testing and Materials*, Vol. 53, 1953 pp. 963-975.

16. Verbeck, G. J., and W. E. Hass. Dilatometer Method for Determination of Thermal Efficient of Expansion of Fine and Coarse Aggregate. *Highway Research Board*, Proceedings of the Thirtieth Annual Meeting, Jan. 9-12, 1951 pp. 187- 192.

17. Thermal Coefficient of Portland Cement Concrete. http://www.tfhrc.gov/pavement/pccp/thermal.htm, accessed 13 August 2004.

18. Dossy, T., B. F. McCullough, and A. Dumas. *Effects of Aggregate Blends on the Properties of Portland Cement Concrete Pavements*. Research Report 1244-8, Center for Transportation Research, The University of Texas at Austin, August 1994.

19. Gnomix pvT High Pressure Dilatometer. http://www.datapointlabs.com/ExpCapShowDetails.asp?InstId=10 accessed 4 September 2004.

20. *Handbook of Chemistry and Physics*. 71st Ed., CRC Press, Boca Raton, Florida, 1990-1991.

21. Shon, C. S., S. Lim, A. K. Mukhopadhyay, D. G. Zollinger, and S. L. Sarkar. New Aggregate Characterization Tests for Thermal and ASR Reactivity Properties. *Proceedings, ICAR 10th Annual Symposium*, April 2002.

22. Ahrens, T. J., *Mineral Physics and Crystallography*, *A Handbook of Physics Constants*. AGU Reference Shelf 2,American Geophysical Union, Washington, D.C. 1995.

23. Mindess, S., and J. F. Young. *Concrete*. Prentice Hall, Inc., Englewood Cliffs, New Jersey, 1999.

APPENDIX A

RELATIONSHIP BETWEEN THE COEFFICIENT OF LINEAR

THERMAL EXPANSION AND THE COEFFICIENT OF

VOLUMETRIC THERMAL EXPANSION

The coefficient of linear thermal expansion and the coefficient of volumetric thermal expansion are designated by α and γ, respectively. When the temperature increases by ΔT, the volume of a body expands from V_1 to V_2. Any length within the body expands from L_1 to L_2. The coefficients α and γ are defined as follows:

$$L_2 = L_1 \times (1 + \alpha \Delta T)$$

$$V_2 = V_1 \times (1 + \gamma \Delta T)$$

The relationship between α and γ is:

$$\gamma = 3\alpha$$

This relationship holds for a body of any regular and irregular shapes. The relationships for the cylinder, and for any irregular shape are verified as follows.

CYLINDER

The volume of a cylinder with radius of r and height of h is:

$$V_1 = \pi r^2 h$$

After thermal expansion, the radius becomes $r\,(1+a\Delta T)$ and the height becomes $h\,(1+a\mathrm{D}T)$, therefore, the volume of the cylinder becomes:

$$V_2 = \pi r^2 (1 + \alpha \Delta T)^2 h (1 + \alpha \Delta T)$$
$$= \pi r^2 h (1 + \alpha \Delta T)^3$$
$$= \pi r^2 h (1 + \alpha^3 \Delta T^3 + 3\alpha \Delta T + 3\alpha^2 \Delta T^2)$$
$$\gamma = \frac{V_2 - V_1}{V_1 \Delta T} = \alpha^3 \Delta T^2 + 3\alpha + 3\alpha^2 \Delta T$$

Since $3\alpha^2 \Delta T$ and $\alpha^3 \Delta T^2$ are much smaller than 3α, they can be neglected and the above equation becomes:

$$\gamma = 3\alpha$$

IRREGULAR SHAPE

For an irregular shape, the volume of a body can be obtained by summing up all the infinitesimal cubics, that is, triple integral:

$$V_1 = \iiint_\Omega dV = \iiint_\Omega dx\,dy\,dz$$
$$V_1 = V$$

Where Ω defines the boundary of the volume. After thermal expansion, the length element dx becomes $(1+\alpha \Delta T)dx$, dy becomes $(1+\alpha \Delta T)dy$, dz becomes $(1+ \alpha \Delta T)dz$, and then the volume element dV becomes $(1+\alpha \Delta T)^3 dV$. Therefore, the volume of the body becomes:

$$V_2 = \iiint_\Omega (1 + \alpha \Delta T)^3 dV$$
$$= (1 + \alpha \Delta T)^3 \iiint_\Omega dV$$
$$= (1 + \alpha \Delta T)^3 V$$

Where since $(1+ \alpha \Delta T)^3$ is a constant, it is moved out of the integral. Therefore, the volumetric coefficient of thermal expansion is:

$$\gamma = \frac{V_2 - V_1}{V_1 \Delta T} = \alpha^3 \Delta T^2 + 3\alpha + 3\alpha^2 \Delta T$$

Since, α is a small quantity, $3\alpha^2 \Delta T$ and $\alpha^3 (\Delta T)^2$ are much smaller than 3α. For example, with $\alpha = 6 \times 10^{-6}$/°C and $\Delta T = 10$ °C, $3\alpha = 1.8 \times 10^{-5}$/°C, while $3\alpha^2 \Delta T = 1.08 \times 10^{-9}$/°C and $\alpha^3 (\Delta T)^2 = 2.16 \times 10^{-14}$/ °C. Therefore, $3\alpha^2 \Delta T$ and $\alpha^3 (\Delta T)^2$ can be neglected in the above equation, and the volumetric and linear coefficients of thermal expansion, γ and α, have the following precise relation:

$$\gamma = 3\alpha$$

This relation is valid for a body of any shape.

APPENDIX B

CALIBRATION PROTOCOL FOR THE DILATOMETER

Following are the guidelines for calibration of dilatometer.

1. Run the device three times with distilled water to establish the gamma flask(γ_f) and its coefficient of variation (COV)

- (COV $= \dfrac{\sigma}{\overline{X}}$; standard deviation divided by the mean) where the standard deviation is based on a minimum of three consecutive tests.

- Recommended maximum. acceptable limit for the COV of the gamma flask is 1.5 percent

2. Run the device three times with a standard reference material (e.g., glass) to establish the correction factor for Δh and its COV based on a minimum of three consecutive tests:

- The correction factor for Δh is the average of three ratios is determined from the tests by dividing the Δh of each test and the Δh to exactly match the CoTE of the reference material. Use the 'Δh' correction factor for all aggregate CoTE tests.

- Recommended maximum limit for the COV of the Δh correction factor is 1.5 percent.

- By fixing the limits for steps 1 and 2, the variability from test to test will be limited to an acceptable range. If the specified COV limits are not met, then repeat the test until the measured COV falls below the required limit.

3. Run the device three times with any aggregate material (e.g., sandstone) to determine aggregate CoTE and its actual CoTE COV:

- Calculated CoTE COV is based on the COV of the gamma flask and correction factor for Δh from spread sheet.

- Assign correction factor (if necessary) for calculated CoTE COV in order to match the actual aggregate CoTE COV determined from the three tests (this value is expected to be less than 5percent).

- Use this correction factor to adjust the calculated CoTE COV from the spreadsheet for future tests.

Note: Repeat the calibration process every 30 tests or six months. Tests of highly porous fine-grained sedimentary rocks (e.g., limestone, sandstone, etc.) must be checked for re-saturation when the aggregate is held at 10ºC at the beginning of the test and at the end of the test when the sample is held at 50ºC. The Δh used to calculate the CoTE for these types of aggregates must reflect the effects of re-saturation.

APPENDIX C

Variance Analysis

$$\gamma_f = \gamma_w - \frac{\Delta h A_t}{V_{f10}\Delta T} - \frac{V_{a10}}{V_{f10}}\gamma_w + \frac{V_{a10}}{V_{f10}}\gamma_a$$

$$\gamma_a = \frac{1}{V_{a10}}\left[\frac{\Delta h A_T}{\Delta_T} + V_{a10}\gamma_w - (\gamma_w - \gamma_f)V_{f10}\right]$$

$$V_{a10} = V_a[1 - \Delta T\gamma_a]$$

$$V_{f10} = V_{w10} + V_{a10}$$

$$Var[\gamma_a] = f(\Delta h V_a \gamma_f \gamma_w) = X_i$$

$$= \sum\left(\frac{\partial\gamma_a}{\partial X_i}\right)VarX_i + \sum\sum\frac{\partial\gamma_u}{\partial X_i}\sigma_i\frac{\partial\gamma_u}{\partial X_i}\rho_{ij}$$

$$VarV_a = \left(\frac{\partial Va}{\partial W}\right)^2 Var(W) = \left(\frac{1}{G\gamma w}\right)^2 (Cov(W)\overline{W})^2$$

$$Var\,\gamma_f = (COV(\gamma_f)\overline{\gamma_f})^2$$

$$Var\,\gamma_w = (COV(\gamma_w)\overline{\gamma_w})^2$$

$$Var\,\Delta h = (COV(\Delta h)\overline{\Delta h})^2$$

$$Var\,\gamma_a = \left[\frac{1}{V_a}\cdot\frac{A_T}{\Delta T}\right]^2 Var\,\Delta h + VarV_a\left[\frac{\gamma w - \gamma a}{V_a}\right]^2 VarV_a$$

$$+ \left[\frac{V_f}{V_a}\right]^2 Var_f + \left[\frac{1}{V_a}(V_a - V_f)\right]^2 Var\,\gamma_w$$

$$Var\,\gamma_a = \frac{1}{V_a^2}\left[\left(\frac{A_T}{\Delta T}\right)^2 Var(\Delta h) + (\gamma_w - \gamma_a)^2 Var(V_a)\right.$$
$$\left.+ (V_f)^2 Var(V_f) + (V_a - V_f)^2 Var\,\gamma_w\right]$$

$$+ \rho(V_{a10})^2\left(\frac{At}{\Delta T}\right)\sqrt{Var\,\Delta h} + (V_{w10} + V_{a10})\sqrt{Var\,\gamma_f}$$

Where V = total inner volume of the flask,

V_w = volume of water in the flask,

V_f = volume of the flask,

V_{a10} = volume of aggregate in the flask,

γ_a = coefficient of volumetric thermal expansion of aggregate,

γ_w = coefficient of volumetric thermal expansion of water, and

γ_f = coefficient of volumetric thermal expansion of flask,

A = inner sectional area of tower,

Δh = rise of the water surface inside the tower,

ΔT = temperature increase from T_1 to T_2.

APPENDIX D

Guidelines for Vacuuming

1. Wash the aggregates thoroughly with distilled water to remove silts, clays, and other fine materials. Select the required quantity of aggregate for the test and immerse in distilled water.

2. Soak the washed aggregates overnight in a container to ensure a high degree of saturation using distilled water.

3. After twenty four hours, transfer the aggregates to a Rice container (used to determine the specific gravity of the material by the Rice method). Place a vacuum (29 inches of mercury) on the container for 15 minutes to remove air trapped between the aggregate particles.

4. Find the specific gravity of aggregates and volume of aggregates using rice method.

5. Transfer the aggregates from the Rice container to the dilatometer very carefully after the dilatometer has been half-filled with distilled water to ensure that there is no air trapped between the aggregate particles.

6. After ensuring against possible leakage, for less porous, coarse-grained, hard, and compact aggregates (e.g., hard, compact, and fresh sandstone, granite, some gravel, and marble) and concrete continue vacuuming for the next 60 minutes while checking that the pressure gage needle does not fluctuate and that the mercury level in the cylinder is near zero. Deviation from these conditions suggests possible leakage. An additional period of vacuuming may be required in case of highly porous, fine-grained, weathered sedimentary rocks (e.g., limestone, sandstone etc.). In case of standard reference materials (e.g., glass, copper, steel, etc.) and water, experience has indicated 45 minutes is sufficient to reduce the air bubble flow to a negligible level.

7. At the completion of each 15 minute vacuuming and vibration period, note the intensity of the flow of air bubbles through the window in the tower before stopping. Intensity may vary from sample to sample but it is recommended to continue the vacuuming until the flow of air bubbles is reduced to a negligible level.

8. During the vacuuming process, it is helpful to apply vibration to the dilatometer. A variable speed Gilson Vibro-Deairator (SGA-5R) was used at TTI. A specific modification adapted the dilatometer to fit on the Vibro-Deairator. Maximum vibration should be applied during the vacuuming process. The effectiveness of the vacuuming de-airing can be monitored by observing the air bubble flow through the window in the tower.

APPENDIX E

Sample Preparation

A sampling protocol is introduced to obtain a representative powder sample; following are the steps involved.

1. Thoroughly wash sample to remove foreign materials (i.e., soil, organics, etc.).

2. Visually inspect the samples with a magnifying glass to judge the aggregate heterogeneity. Aggregate consisting of mainly one type of particles with respect to shape, color, and texture are considered to be as homogeneous (e.g., crushed limestone). On the other hand, aggregate with different types of particles with respect to shape, color, grain size, and texture are considered to be heterogeneous (e.g., gravel). Accurate judgment of heterogeneity is necessary for selecting suitable methods in the following steps.

3. Cone and quarter the sample; the number of cycles of cone and quartering depend on amount of sample needed and level of heterogeneity within the sample, as suggested below (for one bag of sample, i.e., 50 lb):
   - 1 cycle for highly heterogeneous samples, e.g., gravel.
   - 2 cycles for intermediate samples, e.g., impure limestone, sandstones, etc.
   - 3 cycles for homogeneous samples, e.g., pure limestone.

4. Dry the selected amount of sample overnight in oven at 60°C.

5. Crush the entire sample using a jaw crusher or similar type of device.

6. Cone and quarter the crushed sample. The Number of cycles is determined as follows:

- 3 cycles for highly heterogeneous samples because the selected amount before crushing is high.

- 1 or 2 cycles for homogeneous or less heterogeneous samples.

7. Grind the entire sample using a powdering device (e.g., pestle and mortar for small quantities of sample or ball mill for larger quantities of sample particularly, in the case of highly heterogeneous samples) to pass through a number 200 sieve (75 μm).

8. Analyze powder samples by XRF to determine the bulk chemistry.

APPENDIX F

Derived Formulae from Stoichiometric Equations of Minerals to Calculate Weight Percentages of Minerals from Bulk Chemical Analysis by Method I.

Minerals	Chemical formula of minerals	Formulas to calculate mineral weight % based on equations in column 4	Stoichiometric equations
Dolomite (g), Do	$(Ca,Mg)(CO_3)_2$	$= MgO \times 4.5752$*	$CaMg(CO_3)_2 \rightarrow CaO + MgO + 2CO_2$
Albite (g), Ab	$NaAlSi_3O_8$	$= Na_2O \times 8.46$*	$Na_2Al_2Si_6O_{16} \rightarrow Na_2O + Al_2O_3 + 6SiO_2$
Orthoclase (g), Or	$KAlSi_3O_8$	$= K_2O \times 5.80$*	$K_2Al_2Si_6O_{16} \rightarrow K_2O + Al_2O_3 + 6SiO_2$
Anorthite (g), An	$CaAl_2Si_2O_8$	$= (Al_2O_3 - Ab \times 0.1944 - Or \times 0.1832) \times 2.7287$*	$CaAl_2Si_2O_8 \rightarrow CaO + Al_2O_3 + 2SiO_2$
Quartz (g), Qtz	SiO_2	$= SiO_2 - Ab \times 0.6874 - Or \times 0.6595 - An \times 0.4363$	
Calcite (g), Cc	$CaCO_3$	$= (CaO - Do \times 0.3041 - An \times 0.2016) \times 1.785$*	$CaCO_3 \rightarrow CaO + CO_2$
Magnetite (g), Mt	Fe_3O_4	$= Fe_2O_3 \times 1.4499$*	$Fe_3O_4 \rightarrow FeO + Fe_2O_3$

*ratio of mineral's molecular weight to that particular oxide's molecular weight

Sequential Allotment of Elemental Oxide Weight percent to Mineral Weight Percentages by Method II.

Calculation of molecular proportion (MP): divide the weight percentage (wt%) of each oxide by its molecular weight to find the molecular proportion of that oxide			
Minerals	Chemical Formula	Equations to calculate MP for minerals	Residual elemental oxide weight % after formation of a particular mineral
Apatite	$Ca_5(PO_4)(OH,F,Cl)$	= MP of P_2O_5	$CaO_I = CaO_t - 3.33 \times$ MP for apatite
Ilmenite	$FeTiO_3$	= MP of TiO_2 if $FeO > TiO_2$	$FeO_I = $ MP of $FeO_t -$ MP of TiO_2
Orthoclase (K-feldspar)	$KAlSi_3O_8$	= MP of K_2O	Al_2O_3 (I) = MP of $Al_2O_{3(t)} -$ MP of K_2O SiO_2 (I) = MP of $SiO_{2(t)} - 6 \times$ MP of K_2O
Albite (Na-feldspar)	$NaAlSi_3O_8$	= MP of Na_2O	Al_2O_3 (II) = Al_2O_3(I) – MP of Na_2O SiO_2(II) = SiO_2(I) $- 6 \times$ MP of Na_2O
Anorthite (Ca-feldspar)	$CaAl_2Si_2O_8$	= Al_2O_3(II) if $CaO_I > Al_2O_3$(II)	$CaO_{II} = CaO_I - Al_2O_3$(II) SiO_2(III) = SiO_2(II) $- 2 \times Al_2O_3$(II)
Anorthite	$CaAl_2Si_2O_8$	= CaO_I if $CaO_I < Al_2O_3$(II)	Al_2O_3(III) = Al_2O_3(II) – CaO_I SiO_2(III) = SiO_2(II) $- 2 \times CaO_I$
Corundum	Al_2O_3	= Al_2O_3(III)	
Magnetite	Fe_3O_4	= FeO_I if $Fe_2O_{3(t)} > FeO_I$	Fe_2O_3(I) = $Fe_2O_{3(t)} - FeO_I$
Magnetite	Fe_3O_4	= MP of $Fe_3O_{4(t)}$ if $Fe_2O_{3(t)} < FeO_I$	FeO(II) = $FeO_I - Fe_3O_{4(t)}$
Hematite	Fe_2O_3	= Fe_2O_3(I)	
Diopside (Pyroxene)	$(Ca,Mg)Si_2O_6$	= CaO_{II}	$(MgO + FeO)_R$ after diopside $= (MgO_t + FeO_{II}) - CaO_{II}$ SiO_2(IV) $= SiO_2$(III) $- 2 \times CaO_{II}$
Hypersthene (Pyroxene)	$(Fe,Mg)SiO_3$	= $(MgO+FeO)_R$ if diopside is "YES"	SiO_2(V) = SiO_2(IV) – MP for hypersthene
Hypersthene	$(Fe,Mg)SiO_3$	= $(MgO_t + FeO_{II})$ If diopside is "NO"	SiO_2(V) = SiO_2(IV) – MP for hypersthene
Quartz	SiO_2	= SiO_2(V)	
Multiplication of the above molecular proportions assigned to the respective phases by their molecular weight will give the weight % of respective minerals.			

MP – Molecular proportion, t / (t) – total

APPENDIX G

Item 421 Special Provision

421.2. Materials.

E. aggregate.

1. Coarse aggregate. *Coefficient of thermal expansion (CoTE) of coarse aggregate shall not exceed the values specified by engineer when tested in accordance with Test Method Tex-xxx. The Test method Tex-xxx is based on two approaches i.e., direct measurement by Dilatometer (Tex-xxx-A) and prediction by mineralogical modeling (indirect, Tex-xxx-B)). The sampling of coarse aggregate for CoTE measurement shall be done in accordance with test method Tex-yyy. CoTE of one coarse aggregate sample per 2000 ton of aggregate use shall be tested in accordance with Test Method Tex-xxx-B and CoTE of one coarse aggregate sample per 12,500 ton of aggregate use shall be tested in accordance with Test Method Tex-xxx-A.*

421.9. Quality of concrete. *Concrete CoTE shall be predicted in accordance with the Test Method Tex-xxx-C where determined CoTE of coarse aggregate and standard mortar by Test Method Tex-xxx and volume fractions of coarse aggregate and mortar from mixture proportions are the primary inputs. If the sand is other than the conventional silica sand then mortar CoTE in Test Method Tex-xxx-C shall be adjusted. The predicted concrete CoTE in accordance with the Test Method Tex-xxx-C shall conform to the specified range for specific project. Any deviation of concrete CoTE shall be adjusted by slight change of mixture proportion within acceptable limit.*

VITA

Siddharth Neekhra was born in Madhya Pradesh India. He received Bachelor of Engineering degree in civil engineering in 2001 from the Government Engineering College Raipur, India.

Mr. Neekhra began his graduate studies at Texas A&M University in January 2002. While attending Texas A&M University, he was employed as a graduate research assistant by Texas Transportation Institute and as a graduate teaching assistant by the Department of Civil Engineering. He received his Engineer in Training Certificate from Texas in October 2003.

Permanent Address:
126 Sunder Nagar
Raipur Chhattisgar
Email: neekhra@hotmail.com